JOURNAL OF GEOPHYSICAL RESEARCH, VOL. 113, B03204, doi:10.1029/2007JB005208, 2008

Reconstruction of the Talkeetna intraoceanic arc of Alaska through thermobarometry

Bradley R. Hacker,[1] Luc Mehl,[1,2] Peter B. Kelemen,[3] Matthew Rioux,[1,4] Mark D. Behn,[5] and Peter Luffi[6,7]

Received 6 June 2007; revised 21 August 2007; accepted 10 December 2007; published 7 March 2008.

[1] The Talkeetna arc is one of two intraoceanic arcs where much of the section from the upper mantle through the volcanic carapace is well exposed. We reconstruct the vertical section of the Talkeetna arc by determining the (re)crystallization pressures at various structural levels. The thermobarometry shows that the tonalites and quartz diorites intruded at ~5–9 km into a volcanic section estimated from stratigraphy to be 7 km thick. The shallowest, Tazlina and Barnette, gabbros crystallized at ~17–24 km; the Klanelneechena Klippe crystallized at ~24–26 km; and the base of the arc crystallized at ~35 km depth. The arc had a volcanic:plutonic ratio of ~1:3–1:4. However, many or most of the felsic plutonic rocks may represent crystallized liquids rather than cumulates so that the liquid:cumulate ratio might be 1:2 or larger. The current 5- to 7-km structural thickness of the plutonic section of the arc is ~15–30% of the original 23- to 28-km thickness. The bulk composition of the original Talkeetna arc section was ~51–58 wt % SiO_2.

Citation: Hacker, B. R., L. Mehl, P. B. Kelemen, M. Rioux, M. D. Behn, and P. Luffi (2008), Reconstruction of the Talkeetna intraoceanic arc of Alaska through thermobarometry, *J. Geophys. Res.*, *113*, B03204, doi:10.1029/2007JB005208.

1. Introduction

[2] The Talkeetna arc is one of two intraoceanic arcs on Earth where rocks from the upper mantle tectonite at the base of the arc through sediments capping the volcanic carapace are well exposed (Figure 1) [*Burns*, 1985; *DeBari and Coleman*, 1989]. The overarching goal of this study is to reconstruct the vertical section of the Talkeetna arc by determining the (re)crystallization pressures at various structural levels through thermobarometry. The main questions we seek to address are: What was the arc thickness? What was the arc P-T gradient? How much of the arc was removed by deformation and how much now remains? What is the bulk composition of the reconstructed arc's bulk composition? This information is crucial if the Talkeetna arc is to be used as an archetypal cross section for purposes as diverse as understanding the evolution of the Earth's crust, assessing rates and mechanisms of arc growth, and understanding the tectonic history of arcs in general. It is especially important to make thermobarometric estimates because of the structural thinning that occurred during and after accretion of the arc.

[3] The Talkeetna arc was active from 200 Ma to at least 180 Ma, and accreted to the North America margin by the Late Jurassic or Early Cretaceous [*Burns*, 1985; *Plafker et al.*, 1989; *Rioux et al.*, 2003, 2007]. It is exposed as a series of volcanic and plutonic bodies that comprise the Peninsular terrane of south central Alaska. This article focuses on the Chugach and Talkeetna Mountains (Figure 1). Exposures in these areas include all the types of rocks that comprise a magmatic arc: volcaniclastic rocks, hypabyssal and plutonic rocks, and mantle peridotite [*Burns*, 1985; *DeBari and Coleman*, 1989; *Plafker et al.*, 1989; *Mehl et al.*, 2003; *Clift et al.*, 2005a; *Greene et al.*, 2006]. The present structural thickness of the plutonic section of the arc is 5–7 km, but the section is transected by numerous faults, making reconstruction of the arc problematic. Along its southern margin, the arc is structurally juxtaposed with the younger McHugh accretionary complex along one of the many faults in the 5–10 km wide Border Ranges fault system [*Pavlis*, 1982; *Little and Naeser*, 1989]. This fault system, interpreted as a paleosubduction thrust [*Clift et al.*, 2005b], was reactivated in the Cenozoic as a strike-slip fault with hundreds of kilometers of offset [*Pavlis and Roeske*, 2007]. A klippe of arc plutonic rocks is exposed south of the Border Ranges fault zone in the Klanelneechena area [*Winkler et al.*, 1981].

2. Methodology

[4] To reconstruct the vertical section of the Talkeetna arc, we determined the igneous crystallization or metamor-

[1]Department of Earth Science, University of California, Santa Barbara, California, USA.
[2]Now at Woods Hole Oceanographic Institution, Woods Hole, Massachusetts, USA.
[3]Lamont-Doherty Earth Observatory, Earth Institute at Columbia University, Palisades, New York, USA.
[4]Now at Department of Earth, Atmospheric and Planetary Sciences, Massachusetts Institute of Technology, Cambridge, Massachusetts, USA.
[5]Woods Hole Oceanographic Institution, Woods Hole, Massachusetts, USA.
[6]Department of Geological and Planetary Sciences, California Institute of Technology, Pasadena, California, USA.
[7]Now at Department of Earth Science, Rice University, Houston, Texas, USA.

0148-0227/08/2007JB005208$09.00

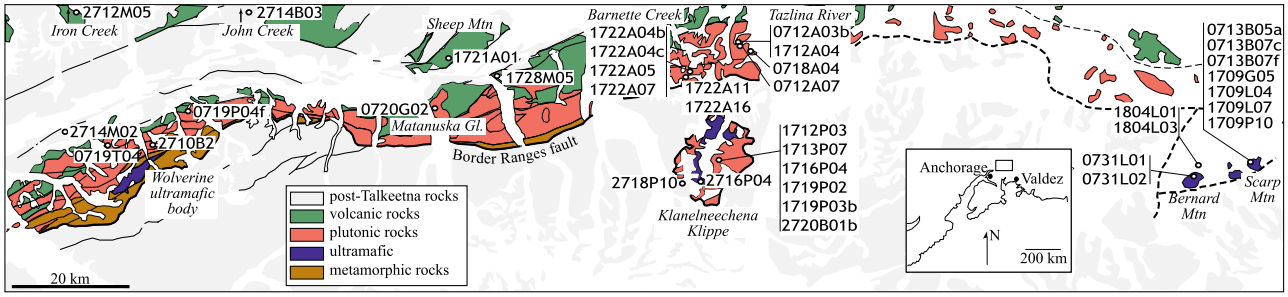

Figure 1. The Talkeetna arc in the Chugach Mountains consists of volcanic rock, plutonic rock, ultramafic rock, and metamorphic rocks (map after *Winkler et al.* [1981] and *Winkler* [1992]). The southernmost Talkeetna Mountains project into the NW corner of the map.

Table 1. Sample Locations[a]

Sample	Description	Minerals	UTM	
0713B05a	Calcsilicate vein from Scarp Mtn	gar cpx plg sph cc	0611426	6835402
0713B07c	Garnet gabbronorite from Scarp Mtn	gar hb cpx opx plg	0611159	6835499
0713B07f	Garnet gabbro from Scarp Mtn	gar hb cpx plg	0611159	6835499
0718A04	Hornblende gabbronorite from Tazlina	hb cpx opx plg	0521911	6851315
0719P04f	Garnet amphibolite from Wolverine/Caribou Cr	gar hb plg qz	0424895	6841025
0719T04	Tonalite near Wolverine	hb bio sphene plg kfs qz ox	0410814	6837329
0720G02	Quartz diorite from Matanuska Glacier	hb bio sph plg kfs qz ox	0469477	6843396
0731L01	Garnet gabbronorite from Bernard Mtn	gar hb cpx opx plg	0599421	6829438
0731L02	Garnet gabbronorite from Bernard Mtn	gar hb cpx opx plg qz	0599421	6829438
1709G05	Garnet amphibolite from Scarp Mtn	gar hb plg	0610924	6835555
1709L03a	Garnet gabbro from Scarp Mtn	gar hb cpx plg	0610865	6835510
1709L04	Garnet gabbro from Scarp Mtn	gar hb cpx plg	0610375	6835455
1709L07	Garnet gabbro from Scarp Mtn	gar hb cpx plg	0611027	6835618
1709P10	Garnet gabbro from Scarp Mtn	gar hb cpx plg	0610581	6835775
1709P11	Two-pyroxene spinel gneiss from Scarp	cpx opx spl plg	0610499	6835729
1710A04b	Hornblende gabbronorite from Scarp Mtn	hb cpx opx plg	0610997	6835362
1710A04d	Hornblende gabbronorite from Scarp Mtn	hb cpx opx plg	0610997	6835362
1710A04e	Hornblende gabbronorite from Scarp Mtn	hb cpx opx plg	0610997	6835362
1710P10	Two-pyroxene spinel from Sheep	cpx opx spl plg	0605864	6829407
1712A03b	Hornblende gabbronorite from Tazlina	hb cpx opx plg	0518764	6853618
1712A04	Hornblende gabbronorite from Tazlina	hb cpx opx plg	0518808	6853291
1712A07	Hornblende gabbronorite from Tazlina	hb cpx opx plg	0518911	6852088
1712P03	Garnet gabbronorite from Klanelneechena	gar opx cpx plg qz	0514629	6830965
1713P07	Garnet norite from Klanelneechena	gar hb opx plg	0512537	6832707
1716P04	Calcsilicate vein from Klanelneechena	gar cpx cc plg qz	0515960	6830448
1719P02	Garnet norite from Klanelneechena	gar opx qz	0514819	6831246
1719P03b	Calcsilicate vein from Klanelneechena	gar cpx cc plg qz	0515010	6831247
1721A01	Hornblende gabbronorite from Sheep	hb opx cpx plg qz	0471072	6854357
1722A04b	Hornblende gabbronorite from Barnette Cr	hb cpx opx plg	0510654	6849197
1722A04c	Hornblende gabbro from Barnette Cr	hb cpx plg	0510654	6849197
1722A05a	Hornblende gabbronorite from Barnette Cr	hb cpx opx plg	0510889	6849161
1722A07	Hornblende gabbronorite from Barnette Cr	hb cpx opx plg	0510889	6848864
1722A11	Hornblende gabbronorite from Barnette Cr	hb cpx opx plg	0510122	6846862
1722A16	Hornblende gabbronorite from Barnette Cr	hb cpx opx plg	0510227	6847214
1728M05a	Tonalite from S Fork Matanuska River	hb bio sph plg kfs qz ox	0478494	6846801
1804L01	Calcsilicate vein from Bernard Cr	gar cpx cc plg	060163x	683054x
1804L03	Calcsilicate vein from Bernard Cr	gar cpx cc plg	060153x	683068x
2710B02a	Calcsilicate vein/layer from Wolverine	gar cpx cc plg qz	0419621	6840015
2712M05	Two-mica garnet quartz diorite from Talkeetna Mtns	gar mu bio plg qz	0434615	6915929
2714B03	Calcsilicate layer from John Cr in the Talkeetna Mtns	gar cpx cc plg qz scap	0512906	6828941
2714M02	Tonalite near Wolverine	hb bio sph plg kfs qz ox	0404764	6836991
2716P04	Garnet amphibolite from Klanelneechena	gar hb plg qz	0512906	6828941
2718P10a	Garnet amphibolite beneath Klanelneechena	gar hb mu plg qz	0510258	6829056
2718P10c	Garnet amphibolite beneath Klanelneechena	gar hb mu plg qz	0510258	6829056
2718P10e	Garnet amphibolite beneath Klanelneechena	gar hb mu plg qz	0510258	6829056
2718P10i	Garnet amphibolite beneath Klanelneechena	gar hb mu plg qz	0510258	6829056
2720B01b	Calcsilicate vein/layer from Klanelneechena	gar cpx cc plg qz	0514088	6832003

[a]Abbreviations: bio, biotite; cc, calcite; cpx, clinopyroxene; gar, garnet; hb, amphibole; kfs, K-feldspar; opx, orthopyroxene; ox, Fe-Ti oxide(s); plg, plagioclase; qz, quartz; scap, scapolite; sph, sphene; spl, spinel; Cr, Creek; Mtn, mountain; Mtns, mountains.

Table 2. Bulk Rock Compositions[a]

Sample	SiO_2	TiO_2	Al_2O_3	FeO	MnO	MgO	CaO	Na_2O	K_2O	P_2O_5	Total
0718A04	44.33	0.681	18.12	12.76	0.197	8.57	14.98	0.65	0.01	0.008	100.31
1709G05	40.27	1.944	18.09	16.57	0.241	8.03	12.85	1.55	0.09	0.253	99.89
1709L07	45.20	0.03	29.15	3.18	0.04	5.11	15.68	0.83	0.01	0.02	99.61
1710A04b	46.26	0.122	21.83	6.04	0.120	10.03	14.78	0.88	0.03	0.011	100.11
1710A04D	41.02	1.944	18.10	15.79	0.212	7.55	12.46	2.23	0.15	0.222	99.68
1710A04e	45.73	0.091	21.38	7.22	0.133	10.73	13.61	1.04	0.01	0.006	99.95
1710P10	52.04	0.113	5.07	5.991	0.150	21.71	14.05	0.25	0.01	0.004	99.838
1712A03B	42.77	0.934	17.20	15.81	0.198	8.12	14.06	0.71	0.02	0.007	99.83
1712A04	43.08	0.910	17.44	15.42	0.191	8.41	14.06	0.75	0.01	0.006	100.28
1712A07	43.06	1.173	17.54	17.00	0.260	7.06	12.59	1.17	0.02	0.008	99.88
1712P03	53.48	0.465	20.98	11.13	0.470	1.51	7.74	3.71	0.10	0.303	99.892
1719P02	43.89	0.717	19.88	14.07	0.575	2.94	13.38	2.50	0.28	0.267	98.497
1721A01	45.31	0.819	20.35	11.27	0.187	7.22	13.03	1.16	0.02	0.011	99.38
1722A04b	45.27	0.326	27.21	5.27	0.066	3.33	16.75	1.36	0.02	0.007	99.61
1722A04C	47.07	0.146	28.07	3.52	0.065	3.37	16.97	1.44	0.02	0.006	100.68
1722A05A	49.82	0.226	16.43	9.04	0.204	11.05	12.56	1.14	0.02	0.006	100.50
1722A07	49.97	0.237	14.00	10.22	0.265	14.87	9.73	0.88	0.03	0.054	100.26
1722A11	44.67	1.000	16.35	14.34	0.224	8.76	13.24	1.00	0.01	0.021	99.62
1722A16	49.20	0.434	16.28	10.30	0.234	10.73	12.13	1.16	0.02	0.012	100.50

[a]Determined by XRF at Washington State University.

phic recrystallization pressures of rocks from different structural levels. Analyzed lithologies include garnet-bearing orthogneisses from the base of the arc crust, hornblende gabbronorites from the plutonic section of the arc, calcsilicate screens between plutons, shallow level K-feldspar-bearing plutons, and schists from beneath the Klanelneechena Klippe; the following sections detail the specific approaches used. Descriptions and bulk compositions of the rocks analyzed are presented in Tables 1 and 2. Mineral compositions were measured with a five-spectrometer Cameca SX-50 electron microprobe using a 15-kV beam focused to a 2-μm, 15 nA spot, with reference to natural and synthetic mineral standards. Mineral core and rim compositions are given in Data Set S1 in the auxiliary material.[1] Unless otherwise noted, pressures and temperatures were determined using THERMOCALC 3.1, with the May 2001 database [*Holland and Powell*, 1998]. Determinations for the garnet gabbros were checked using TWQ v1.02 [*Berman and Brown*, 1992], which yielded indistinguishable results. Activities were calculated using the program AX by T. Holland (ftp://www.esc.cam.ac.uk/pub/minp/AX), except for jadeite activities, which were calculated after *Holland* [1990], and spinel activities, which were calculated using an updated version of the *Sack and Ghiorso* [1991] solution model (M. S. Ghiorso, personal communication, 2003).

3. Garnet-Bearing Orthogneisses

[5] Rare garnet-bearing rocks (henceforth referred to as "garnet gabbros") are exposed at the base of the arc crustal section on Bernard and Scarp Mountains and at midcrustal depths in the Klanelneechena Klippe and Wolverine areas. The garnets occur in layered gabbronorites on Bernard Mountain (samples 0731L01, 0731L02); in blocks of gabbronorite enclosed in leucocratic gabbro (0713B07C, 0713B07F), in plagioclase-rich segregations in layered gabbro (1709G05, 1709L03A, 1709L04), and in gabbroic lenses in pyroxenite on Scarp Mountain (1709P10); in layered pyroxene quartz diorites, and hornblende gabbros in the Klanelneechena Klippe (1712P03, 1713P07, 1719P02, 2716P04); and in a metagabbroic rock from the Wolverine area (0719P04f). All the rocks have a foliation defined by variations in phase proportions, but the textures are otherwise granoblastic with little evidence of deformation.

[6] The Scarp and Bernard samples have lower Mg # and Ni than typical Talkeetna gabbronorites and lack the HREE enrichment characteristic of igneous garnet. Most contain 30–40 vol % poikiloblastic garnet (almandine > pyrope > grossular) with pyroxene inclusions, suggesting that garnet grew principally through plagioclase consumption, perhaps in reaction with olivine that was completely consumed; two other samples (0713B07c and 1709L07) have only 1–5 vol % garnet grown over spinel along pyroxene-plagioclase grain boundaries. The Klanelneechena samples have high HREE, indicating that their garnet is magmatic and lower Mg # than other plutonic rocks in the arc section. These features, combined with strong outcrop-scale banding implies that that the Klanelneechena garnet-bearing rocks are restites from melting of relatively evolved volcanic (or plutonic) rocks progressively buried during crustal thickening [*Kelemen et al.*, 2003a]. They contain <10 vol % poikiloblastic garnet (almandine > pyrope = grossular) spatially associated with ilmenite/magnetite.

[7] The garnets at all locations show broad core-to-rim zoning toward lower Mg #, pyroxenes display only near-rim, steep increases in Mg # and Al_2O_3, and plagioclase crystals are unzoned (Figure 2). These patterns are characteristic of cooling. There are no zoning discontinuities or Mn spikes in garnet rims and no textural indicators of garnet resorption. The pyroxenes from the base of the arc are the most aluminous pyroxenes in the arc and the hornblende is the most sodic and aluminous. The plagioclase from the klippe is among the least anorthitic in the arc.

[8] We determined the equilibration pressures and temperatures of these garnet gabbros and diorites using equilibria among garnet, orthopyroxene, clinopyroxene, hornblende, plagioclase and quartz (Figure 3a and Table 3). For the bulk of the samples, equilibrium temperatures and pressures were calculated using net transfer reactions among

[1]Auxiliary materials are available at ftp://ftp.agu.org/apend/jb/2007jb005208.

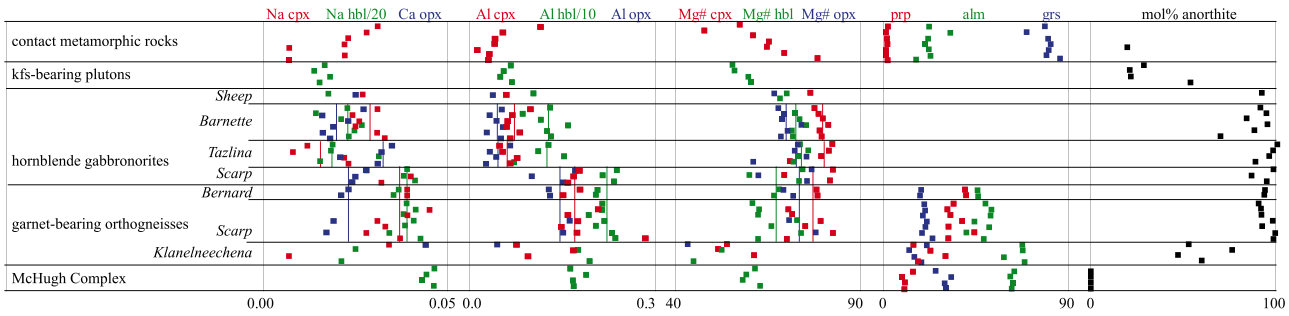

Figure 2. Mineral rim compositions vary systematically throughout the Talkeetna arc. Vertical bars indicate averages parts of the arc section named in italics on the left. Abbreviations are alm, almandine; cpx, clinopyroxene; grs, grossular; hbl, hornblende; kfs, K-feldspar; opx, orthopyroxene; prp, pyrope.

garnet + orthopyroxene (GO), garnet + orthopyroxene + plagioclase + quartz (GOPS), garnet + clinopyroxene + plagioclase + quartz (GADS), garnet + hornblende + plagioclase + quartz (GHPQ), and garnet ± orthopyroxene ± plagioclase ± amphibole ± clinopyroxene. Diffusion models using the multicomponent formulation of *Carlson* [2006], calculated for a range of temperatures and a cooling rate of 40 K/Ma (inferred from thermochronology), show that even the core compositions of these garnets are unlikely to preserve their peak temperature compositions. The absence of any compositional or textural indications of retrograde net transfer reactions, however, suggests that diffusion within garnet was limited to Fe-Mg exchange. Simple models of the effects of such exchange indicate that the peak pressures and temperatures were higher than reported by an unknown amount. For three samples (see Table 3), temperature was estimated using only Fe-Mg exchange; because Fe-Mg exchange continues during cooling to lower temperatures than net transfer reactions, any P-T "point" determined by intersection between these two types of reaction will be in error, with the magnitude of the error increasing with temperature, decreasing cooling rate, decreasing grain size, a_{H2O}, etc.

[9] The mineral core compositions suggest that the two garnet gabbronorites studied at the base of the arc section at Bernard Mountain crystallized at ~875–935°C, 0.9–1.0 GPa, and the four garnet gabbros exposed as mafic pods, thin garnet-bearing bands within layered gabbros, or lenses within pyroxenite on Scarp Mountain indicate conditions of ~890–1010°C and 0.8–1.2 GPa. These P-T conditions are compatible with the position of the garnet-in reaction calculated using Perple_X (pale gray region, Figure 3a). Sample 1709L07 from Scarp, at the high end of the P-T range for this locality, might appear to have given anomalous results, but P-T results from additional garnet-free Scarp Mountains rocks discussed in the next section corroborate these pressures and temperatures. These results corroborate early P-T estimates by *DeBari and Coleman* [1989].

[10] Mineral core compositions in the three garnet-bearing Klanelneechena Klippe samples indicate significantly lower temperatures and pressures of ~704–872°C, 0.7–0.8 GPa. The weighted mean of these analyses is 749 ± 96°C/0.73 ± 0.14 GPa (2σ, MSWD = 0.30). These P-T conditions are compatible with the position of the garnet-in reaction calculated using Perple_X (dark gray line, Figure 3a). The metagabbroic sample from the Wolverine area (0719P04f) near the Border Ranges fault system gave even lower pressure equilibration conditions of 636 ± 95°C and 0.61 ± 0.18 GPa. However, unpublished Sm-Nd isochron data from J. Blusztajn (personal communication, 2000) for this sample suggest a Cretaceous age, indicating that it was reheated or that it is unrelated to the Jurassic Talkeetna arc. An aplitic quartz diorite pegmatite (2712M05) from the central Talkeetna Mountains contains igneous garnet, muscovite and biotite. Application of garnet-biotite thermometry and garnet-biotite-muscovite-plagioclase barometry gives equilibration conditions of 710 ± 75°C and 0.59 ± 0.10 GPa, although, again, these estimates are likely affected by Fe-Mg exchange. These may correspond to crystallization conditions for the phenocryst assemblage, rather than the depth of dike emplacement.

4. Spinel Symplectites in Gabbronorites and Websterites

[11] Spinel-rich orthogneisses and pyroxenites are also common at Scarp and Bernard Mountains. They have higher Ni and Mg # than gabbronorites, positive whole rock Sr and Eu anomalies, and low middle to heavy REE, indicating that they formed from a troctolite protolith (mainly olivine + plagioclase) [e.g., *Miller et al.*, 2007]. The spinel-rich pyroxenites contain elongate ~3 × 3 × 1 cm lenses of clinopyroxene + orthopyroxene + aluminous spinel + hornblende in a coarser olivine-websterite matrix. Some websterites contain minor plagioclase, though olivine and plagioclase have not been observed in contact. The spinel-rich orthogneisses contain plagioclase, two pyroxenes, and hornblende, without olivine. In both types of rock the spinel is generally in symplectitic intergrowth with two pyroxenes. We interpret the symplectites in these samples as having formed by the reaction olivine + plagioclase → orthopyroxene + clinopyroxene + spinel during cooling and/or pressure increase. This reaction terminated with the exhaustion of plagioclase in the pyroxenites and of olivine in the orthogneisses.

[12] We investigated one orthogneiss (1709P11) and one pyroxenite (1710P10). The pyroxenes show only slight zoning (e.g., a decrease in clinopyroxene Al_2O_3 from 5.7 to 5.4% from core to rim), but spinel shows significant variation in all major constituents from $(Mg_{0.6}Fe_{0.4})(Cr_{0.3}Al_{1.7})O_4$ to $(Mg_{0.6}Fe_{0.4})(Fe_{0.1}Cr_{0.4}Al_{1.5})O_4$ in the py-

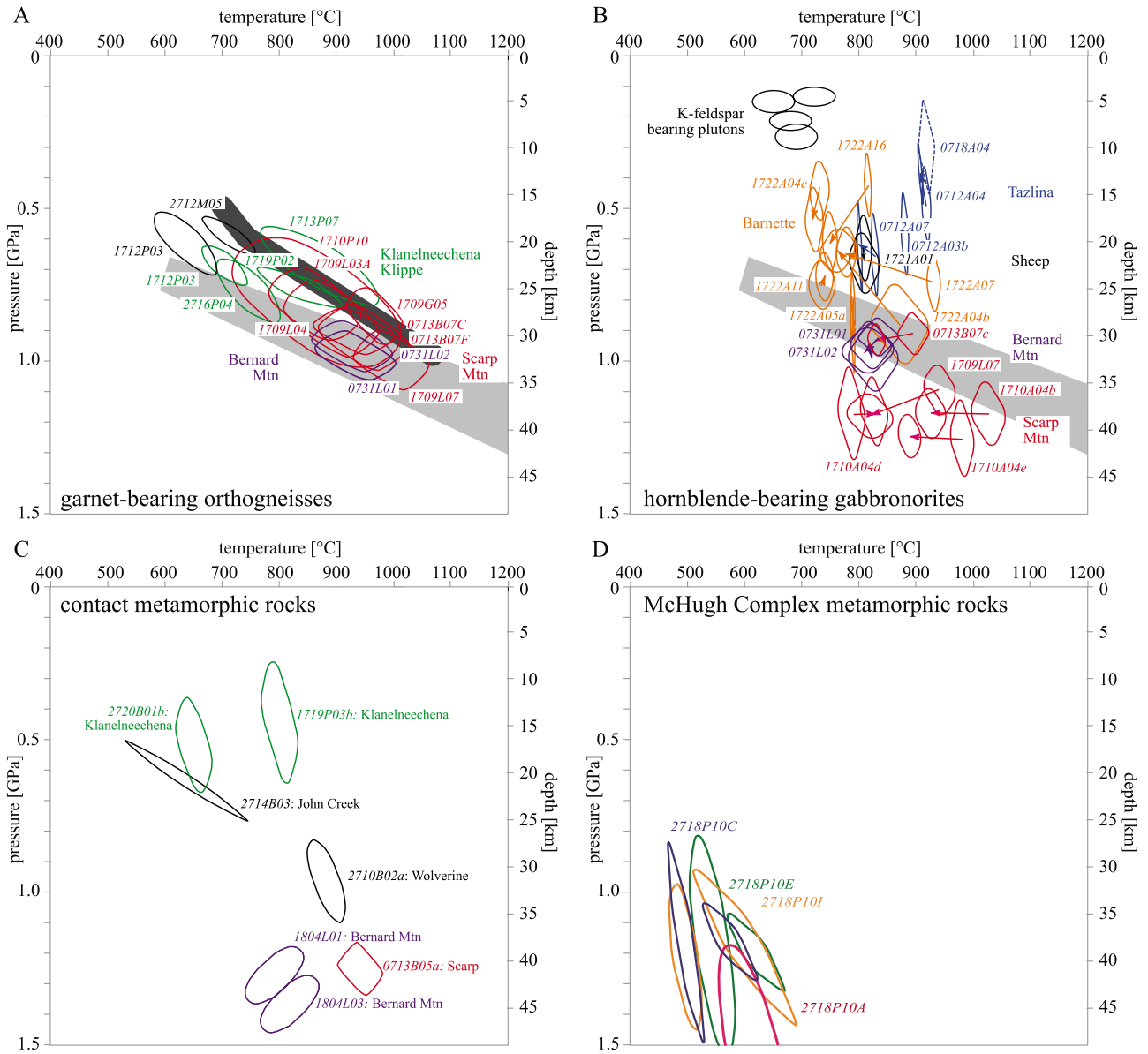

Figure 3. P-T conditions for the Talkeetna arc. Uncertainties are ±0.5σ for clarity. Pressures converted to depth assuming densities of 2.9 and 3.1 g/cm^3 for the volcanic and plutonic sections, respectively [*Behn and Kelemen*, 2006]. Pale gray field shows the garnet-in boundary for Bernard and Scarp Mountain samples calculated using Perple_X; dark gray line shows equivalent for Klanelneechena quartz diorite. (a) Garnet-bearing orthogneisses show equilibration depths of ~20–40 km. (b) Hornblende gabbronorites give equilibration depths of ~5–40 km; K-feldspar bearing plutons crystallized at 5–9 km. Arrows show core-to-rim zoning. Dashed ellipse shows "core" conditions for sample 0718A04. (c) Contact metamorphic rocks show equilibration depths of ~15–45 km; uncertainties shown are for fixed a_{CO2}, which is uncertain (see text). (d) Metamorphic rocks in the McHugh Complex beneath the Klanelneechena Klippe yield equilibration depths of ~30–40 km. Two P-T ellipses are shown for some samples; see the text and Table 4 for an explanation.

roxenite and from $(Mg_{0.7}Fe_{0.3})(Al_{2.0})O_4$ to $(Mg_{0.6}Fe_{0.4})(Cr_{0.1}Al_{1.9})O_4$ in the orthogneiss. Temperatures of 915–975°C are indicated by two-pyroxene solvus thermometry using QUILF [*Andersen et al.*, 1993], whereas Fe-Mg exchange between spinel and orthopyroxene [*Liermann and Ganguly*, 2003] gives, as expected, colder temperatures of 860–875°C. Modeling of pyroxenite phase relations using Domino [*de Capitani and Brown*, 1987] (with the Holland and Powell data set) confirms that igneous crystallization at ~0.1 to 0.6 GPa followed by a pressure increase to ~1 GPa is consistent with our observations (Figure 4).

5. Hornblende Gabbronorites

[13] The greatest challenge in reconstructing the arc section derives from the fact that the bulk of the arc is

Table 3. PT Conditions for Garnet-Bearing Orthogneisses[a]

Sample	T, °C	Method	P ± 1σ, GPa	Method	Cor	Location
0713B07c	931 ± 112	g o c p	0.90 ± 0.12	g h o c p	0.40	Scarp
0713B07f	948 ± 126	g h c p	0.92 ± 0.17	g h c p	0.41	Scarp
0719P04f	636 ± 95	g h c p	0.61 ± 0.18	g h c p	0.77	Wolverine
0731L01	934 ± 111	g h o c p	0.98 ± 0.13	g h o c p	0.43	Bern
0731L02	928 ± 112	g h o c p	0.95 ± 0.13	g h o c p	0.42	Bern
1709G05	967 ± 77	g h p	0.85 ± 0.15	g h p	0.49	Scarp
1709L03a	890 ± 131	g h c p	0.86 ± 0.20	g h c p	0.46	Scarp
1709L04	863 ± 129	g h c p	0.81 ± 0.19	g h c p	0.46	Scarp
1709L07	993 ± 117	g h o c p	1.00 ± 0.14	g h o c p	0.45	Scarp
1709P10	866 ± 240	g h c p	0.81 ± 0.35	g h c p	0.59	Scarp
1712P03	704 ± 68	GC	0.69 ± 0.11	GADS	0.75	Klanelneechena
1713P07	872 ± 169	g h o p	0.69 ± 0.21	g h o p	0.79	Klanelneechena
1719P02	836 ± 121	GO	0.76 ± 0.11	GOPS	0.85	Klanelneechena
2712M05	710 ± 75	GB	0.59 ± 0.10	g b m p	0.81	quartz diorite
2716P04	745 ± 97	g h p q	0.77 ± 0.18	g h p q	0.77	Klanelneechena

[a]A "method" abbreviation indicates that a single reaction was used. GADS, GO, and GOPS defined in text; GB, almandine–pyrope + phlogopite–annite equilibrium; GC, almandine–pyrope + diopside–hedenbergite equilibrium; and separate letters (e.g., "g h o p") indicate that all equilibria involving those minerals (other than the jadeite, glaucophane, and ferro-actinolite endmembers) were used: b, biotite; c, clinopyroxene; g, garnet; h, hornblende; m, muscovite; o, orthopyroxene; p, plagioclase. Cor, correlation coefficient between P and T uncertainties.

composed of plutonic rocks with high-variance assemblages of minerals that span rather small ranges in molar volume. The most promising, relatively low-variance rocks are hornblende gabbronorites, so we used them to provide best estimates of PT conditions. We sampled hornblende gabbronorites near the base of the arc crust on Scarp Mountain and Barnette Mountain and higher in the section along the Tazlina River and Barnette Creek. Typical Talkeetna arc hornblende gabbronorite consists of anhedral-subhedral igneous grains with little deformation; minor (sub)greenschist-facies alteration in the form of chlorite or sericitization is common. In the bulk of the samples, hornblende comprises 2–10 vol % of the rock and ranges from comparable in grain size and habit to pyroxene to smaller than and interstitial to pyroxene. A few samples (0713B07c, 1710A04d, and 1710A04e) contain 20–50 vol % equant to poikilitic hornblende instead. Hornblende textures do not suggest formation as an alteration phase in any of the samples analyzed

[14] All the phases in the hornblende gabbronorites are typically zoned. Plagioclase in all samples is slightly zoned toward lower anorthite rims (with a typical decrease of 5 mol%); it is $\sim An_{80-90}$ in the Scarp Mountain sample and in most Barnette Mountain samples, An_{90-95} at Tazlina, and An_{60-80} in one Barnette sample (Figure 2). Hornblende in all samples is zoned toward Al- and Na-poor rims with higher Mg #; most of the Tazlina hornblendes are less sodic than the Barnette hornblendes, but otherwise similar. Most orthopyroxenes are zoned toward less aluminous and less calcic rims and all clinopyroxenes exhibit rimward decreases in Al and Na and increases in Mg #; the Scarp pyroxenes are the richest in Al and Na. Clinopyroxene Na contents decrease from Scarp to Barnette to Tazlina. The differences in the mineral compositions suggest that the Tazlina, Barnette, and Scarp sections crystallized at successively greater depths. Zoning relationships show that hornblende and clinopyroxene lost Na to plagioclase; orthopyroxene lost Ca to all other phases; and Al moved from orthopyroxene and clinopyroxene to hornblende and plagioclase. This zoning is inferred to have developed during subsolidus reequilibration in response to introduction of fluids or heat from younger intrusions, and during cooling of the arc. The transfer of Na from clinopyroxene into plagioclase and Al from orthopyroxene and clinopyroxene into hornblende and plagioclase indicates a decreasing P/T ratio, whereas the increasing Mg # spread among the ferromagnesian phases indicates cooling.

[15] We calculated pressures and temperatures using a variety of methods to ensure accuracy and redundancy (Figures 3b and 5 and Table 4). The robust clinopyroxene-orthopyroxene calibration in QUILF [*Andersen et al.*, 1993]

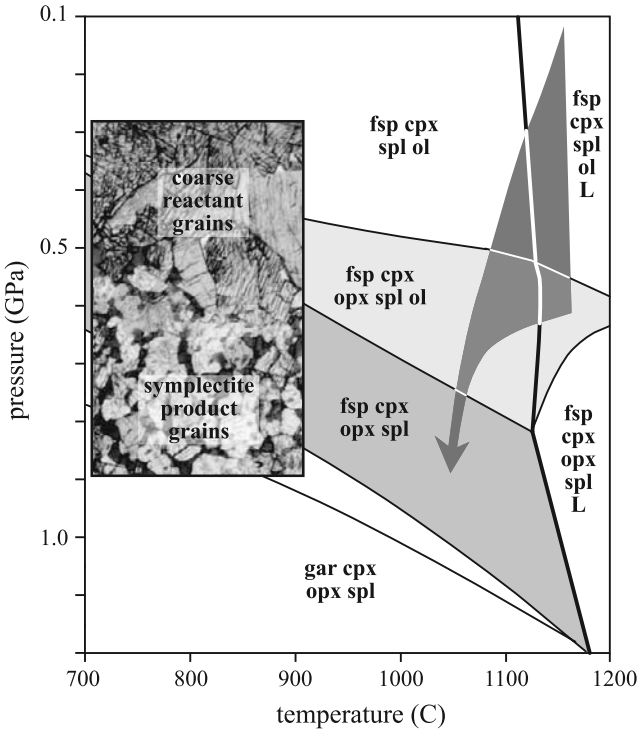

Figure 4. Phase relations for orthogneiss 1709P11, showing pressure-induced consumption of olivine from the igneous assemblage feldspar (fsp) + clinopyroxene (cpx) + orthopyroxene (opx) + spinel (spl) + olivine (ol) ± liquid (L) to produce cpx + opx + spl symplectite. A range of P-T paths compatible with this inferred transformation is shown. Photomicrograph shows typical texture.

is considered to generate the best temperature estimates for rocks of this composition because it considers Fe, Mg, and Ca partitioning and is therefore more resistant to resetting than Fe-Mg exchange (P ± 1σ in Table 4). The simplest way to calculate pressure is to employ the "mode 2" method of THERMOCALC [*Powell and Holland*, 1988], which determines the intersections of equilibria calculated from the activities of mineral end-members. "Mode 2 without quartz" in Table 4 shows the results of this method using all available activities, excepting quartz, which is present in only a few samples. After observing that the activities for hedenbergite, ferrosilite, ferroactinolite, and glaucophane were the most discrepant relative to the mean (presumably because the oxidation state of Fe cannot be determined by electron probe) or had values approaching zero, these activities were removed and the results for "mode 2" in Table 4 were calculated. Finally, pressures were calculated separately for five equilibria that showed the most consistent sample-sample behavior (Figure 5):

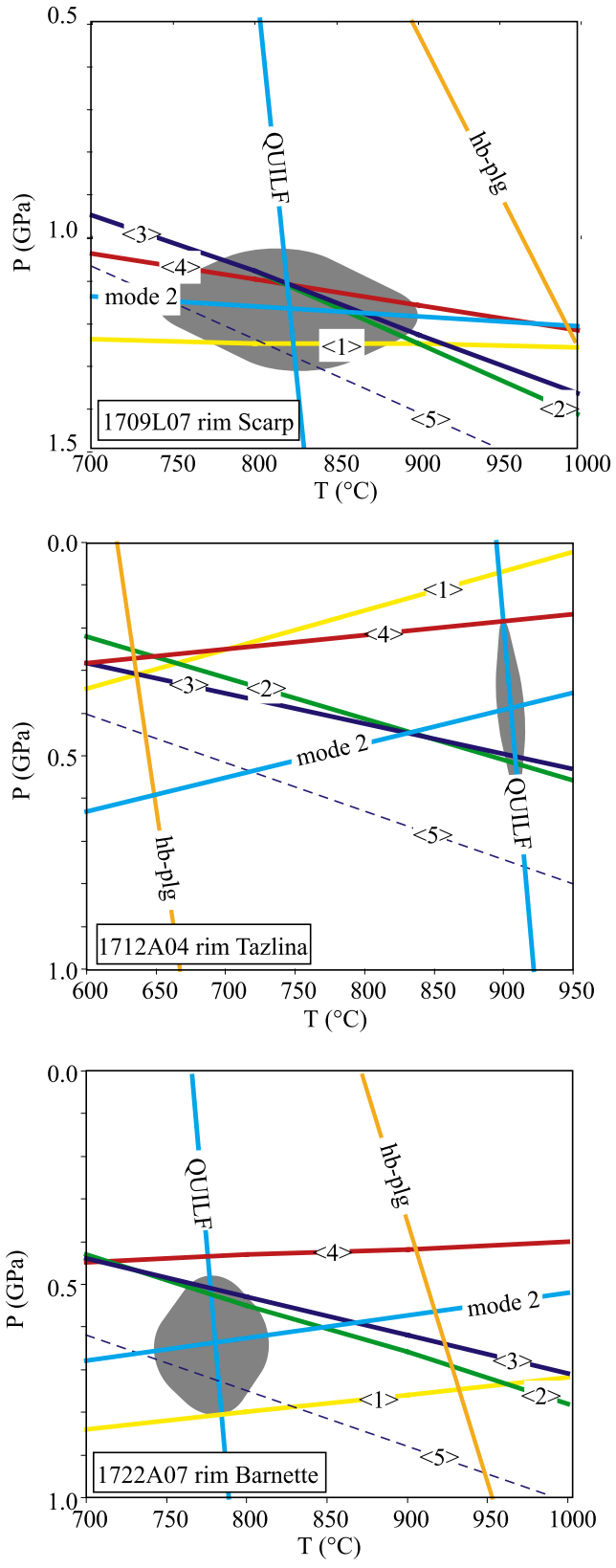

(R1) 2 albite + 5 tschermakite + 8 diopside = 8 anorthite + 3 tremolite + 2 pargasite

(R2) 4 anorthite + pargasite + Mg − Tschermak orthopyroxene = albite + tschermakite + enstatite + 4 Ca-Tschermak clinopyroxene

(R3) tremolite + tschermakite + 8 jadeite = 6 albite + 2 pargasite

(R4) tremolite + Mg-Tschermak in orthopyroxene + 4jadeite = 3 albite + pargasite + enstatite

(R5) albite = jadeite + quartz

Reaction (R1) does not involve orthopyroxene. Reactions (R2) and (R4) require the presence of enstatite and the determination of Tschermak substitutions in pyroxenes, which are uncertain because of limitations in measuring Si and Fe^{3+}. Reaction (R3) does not involve either pyroxene. Reaction (R5) provides only an upper P limit as most rocks lack quartz, but has the advantage that it does not involve amphibole. Intersections of each of these equilibria with the QUILF-determined temperature are for reactions (R1)–(R5) in Table 4, and the mean intersection of all five of these reactions with the QUILF-determined temperature is given for "P ± 1σ" in Table 4.

[16] Because pressures are not typically calculated for hornblende gabbronorites and yet they are crucial for

Figure 5. Three examples of equilibria calculated for hornblende gabbronorites, highlighting the difficulties in accurate P-T determinations for these garnet-free rocks. Labeled equilibria: "QUILF", clinopyroxene-orthopyroxene [*Andersen et al.*, 1993]; "hb-plg", hornblende-plagioclase [*Blundy and Holland*, 1990]; "mode 2," THERMOCALC [*Powell and Holland*, 1988] mode 2 average P-T determination; ⟨1⟩–⟨5⟩, refer to reactions (R1)–(R5) in text. Grey 1σ ellipses show values reported in Table 2.

Table 4. PT Conditions for Gabbro (Norites)

Sample	T ± 1σ,[a] °C	P ± 1σ,[b] GPa	(R1)[c]	(R2)[c]	(R3)[c]	(R4)[c]	(R5)[c]	Mode 2 [d,e]	Mode 2 Without Quartz [d,f]
0713B07c[g] core	895 ± 57	0.91 ± 0.11	0.61	1.15	1.18	0.89	1.4	880 ± 136, 0.91 ± 0.12, 0.40	914 ± 107, 0.92 ± 0.12, 0.45
0713B07c[g] rim	832 ± 31	0.93 ± 0.15	0.92	1.4	1.4	1.0	1.6	777 ± 125, 0.91 ± 0.12, 0.45	759 ± 150, 1.07 ± 0.22, 0.62
0718A04 core	915 ± 26	0.30 ± 0.33	0.10	0.25	0.18	0.30	0.53	628 ± 233, 0.34 ± 0.26,−0.71	835 ± 197, 0.16 ± 0.29, −0.62
0731L01[g] core	830 ± 66	0.92 ± 0.15	1.15	0.84	0.84	0.73	0.97	885 ± 169, 0.92 ± 0.17, 0.00	921 ± 150, 0.92 ± 0.16, −0.01
0731L01[g] rim	820 ± 52	0.99 ± 0.12	0.98	0.85	0.89	0.88	0.97	944 ± 172, 0.99 ± 0.17, 0.09	960 ± 145, 1.00 ± 0.17, 0.03
0731L02[g] core	831 ± 68	0.93 ± 0.11	0.93	0.88	0.71	0.79	0.83	943 ± 156, 0.98 ± 0.14, 0.46,	876 ± 122, 1.10 ± 0.19, 0.60,
0731L02[g] rim	821 ± 89	0.96 ± 0.16	0.92	0.91	0.91	0.92	0.93	960 ± 208, 0.94 ± 0.18, −0.13	733 ± 134, 1.14 ± 0.20, 0.38
1709L07[g] core	935 ± 50	1.09 ± 0.13	1.46	0.90	0.77	0.78	0.98	1123 ± 200, 1.21 ± 1.9, 0.63	1126 ± 116, 1.20 ± 1.6, 0.59
1709L07[g] rim	820 ± 75	1.18 ± 0.14	1.26	1.12	1.12	1.12	1.29	857 ± 151, 1.19 ± 0.15, 0.24	863 ± 126, 1.18 ± 0.15, 0.16
1710A04b core	875 ± 55	1.17 ± 0.20	1.46	1.32	1.32	0.9	1.5	no fit	1047 ± 302, 1.21 ± 0.26, 0.24
1710A04b rim	925 ± 55	1.17 ± 0.17	1.10	1.38	1.45	0.60	1.48	no fit	895 ± 212, 1.16 ± 0.21, 0.21
1710A04d core	780 ± 40	1.17 ± 0.30	1.55	0.91	0.96	0.59	1.03	no fit	1074 ± 432, 1.35 ± 5, 0.46
1710A04d rim	825 ± 35	1.17 ± 0.23	1.58	0.98	0.96	0.93	1.09	997 ± 269, 1.27 ± 0.32, 0.46	1014 ± 164, 1.28 ± 0.32, 0.35
1710A04e core	975 ± 39	1.25 ± 0.24	1.29	1.32	1.39	no fit	1.7	979 ± 307, 1.25 ± 3.1, 0.35	no fit
1710A04e rim	885 ± 37	1.24 ± 0.14	1.37	1.22	1.22	0.91	1.42	943 ± 176, 1.27 ± 1.8, 0.37	no fit
1712A03b rim	880 ± 11	0.59 ± 0.26	0.87	0.18	0.17	0.14	0.34	no fit	1056 ± 293, 0.47 ± 0.33, −0.62
1712A04 core	918 ± 15	0.48 ± 0.24	0.63	0.31	0.34	no fit	0.58	no fit	1052 ± 334, 0.39 ± 0.41, −0.68
1712A04 rim	910 ± 5	0.39 ± 0.2	0.03	0.52	0.51	0.18	0.74	983 ± 349, 0.32 ± 0.36, −0.81	937 ± 308, 0.37 ± 0.33, −0.77
1712A07 core	828 ± 12	0.70 ± 0.27	0.46	0	0.13	no fit	0.25	no fit	948 ± 216, 0.53 ± 0.35, −0.57
1712A07 rim	800 ± 6	0.62 ± 0.31	no fit	0	no fit	no fit	0.18	no fit	813 ± 251, 0.62 ± 0.41, −0.48
1721A01 core	805 ± 28	0.63 ± 0.14	[mgts] [h]	0.48	[mgts]	0.33	= 0.58	702 ± 218, 0.65 ± 0.12, −0.07	906 ± 190, 0.59 ± 0.15, −0.18
1721A01 rim	800 ± 41	0.68 ± 0.19	[mgts]	no fit	[mgts]	0.31	no fit	no fit	no fit
1722A04b core	760 ± 50	0.87 ± 0.27	1.11	0.62	0.62	0.18	0.74	999 ± 403, 0.87 ± 0.37, 0.01	804 ± 273, 0.64 ± 0.25, 0.44
1722A04b rim	755 ± 60	0.65 ± 0.14	0.56	0.33	0.26	0.38	0.48		1031 ± 234, 0.87 ± 0.27, −0.1
1722A04c core	735 ± 33	0.44 ± 0.19	0.40	0.14	0.18	0.36	0.31	891 ± 306 0.30 ± 0.35−0.77	999 ± 217, 0.52 ± 0.26, −0.46
1722A04c rim	725 ± 31	0.53 ± 0.21	[mgts]	0.32	[mgts]	0.14	0.44	1114 ± 463, 0.27 ± 0.42, −0.76	687 ± 97, 0.61 ± 0.15, 0.03
1722A05a core	790 ± 4	0.79 ± 0.18	1.03	0.53	0.53	0.54	0.61	1035 ± 260, 0.75 ± 0.21, −0.19	1018 ± 237, 0.33 ± 0.31, −0.54
1722A05a rim	785 ± 5	0.91 ± 0.27	0.95	0.54	0.42	0.12	0.56	no fit	853 ± 122, 0.92 ± 0.18, 0.30
1722A07 core	930 ± 23	0.74 ± 0.19	1.02	0.74	0.68	0.55	0.90	947 ± 268, 0.73 ± 0.23, −0.35	1023 ± 223, 0.84 ± 0.26, −0.30
1722A07 rim	780 ± 33	0.64 ± 0.17	0.80	0.51	0.51	0.44	0.73	893 ± 237, 0.58 ± 0.23, −0.54	1047 ± 210, 0.71 ± 0.22, −0.31
1722A11 core	735 ± 42	0.65 ± 0.17	0.68	0.24	0.26	0.73	0.35	857 ± 234, 0.58 ± 0.23, −0.55	922 ± 184, 0.58 ± 0.22, −0.45
1722A11 rim	735 ± 30	0.72 ± 0.17	0.91	0.46	0.46	0.46	0.56	979 ± 262, 0.64 ± 0.22, −0.38	696 ± 88, 0.81 ± 0.14, 0.26
1722A16 core	815 ± 11	0.42 ± 0.21	[mgts]	0.39	[mgts]	0.55	0.51	765 ± 225, 0.44 ± 0.22, −0.39	974 ± 188, 0.6.4 ± 0.22, −0.31
1722A16 rim	750 ± 24	0.61 ± 0.19	0.62	0.23	0.20	0.91	0.29	792 ± 230, 0.60 ± 0.21, −0.22	705 ± 96, 0.69 ± 0.16, 0.42

[a]Temperature determined from QUILF.
[b]Pressure determined using THERMOCALC mode 2, excluding activities for hedenbergite, ferrosilite, ferro-actinolite, and glaucophane.
[c]Pressure determined using THERMOCALC and reaction (R1), (R2), (R3), (R4), and (R5), respectively; [mgts], absence of magnesio-Tschermak component in orthopyroxene precludes calculation.
[d]For each row, the first value is T(°C) ± 1σ, second value is P(GPa) ± 1σ, and third value is correlation coefficient.
[e]*P-T* intersection determined using THERMOCALC mode 2, excluding activities for hedenbergite, ferrosilite, ferro-actinolite, and glaucophane; numbers are °C ± 1σ, GPa ± 1σ, and correlation coefficient (all have good values of fit).
[f]*P-T* intersection determined using THERMOCALC mode 2, excluding quartz; numbers are °C ± 1σ, GPa ± 1σ, and correlation coefficient (all have good values of fit).
[g]PT conditions also calculated using garnet (Table 1).
[h]Orthopyroxene does not contain a Mg-Tschermak component.

reconstructing the Talkeetna arc, some comments are in order. The pressures in Table 4 have large absolute uncertainties because of heavy reliance on (1) the activities of amphibole end-members, which are based on poorly known activity models, and (2) knowing the Tschermak components in pyroxene, which cannot be calculated with great accuracy. We require, therefore, a means of assessing the accuracy of the calculated pressures. First, the calculated pressures should be greater than ~0.2 GPa if the hornblende gabbronorites are coeval with or younger than the 7 km thickness of the volcanic section that overlies the gabbronorites [*Clift et al.*, 2005a], and they are. Second, we can compare these results with the pressures calculated for the three hornblende-garnet gabbros described in the previous section (Figure 3b). If uncertainties are ignored, the results show <7% deviation and no systematic displacement to higher or lower pressures than those determined from equilibria including garnet (Figure 6), indicating that the "hornblende gabbronorite" method is reliable.

[17] There is no foolproof method by which one can test whether the mineral core compositions or mineral rim compositions are in equilibrium and which, if either, is to be considered the best indicator of a real P-T condition. Fortunately, for most of the Scarp Mountain and Bernard Mountain samples, this uncertainty makes little difference because the mineral cores and rims yield similar pressures. The Barnette Creek samples, however, show more significant phase zoning; because the P-T conditions derived from their mineral cores are widely scattered and yet the P-T conditions derived from mineral rims form a cluster, we consider the latter to be more reliable. Whether the Barnette core P-T conditions have geologic significance is unknown, but the range in apparent pressures renders this unlikely. One sample from the Tazlina area (0718A04) did not yield rim compositions in apparent equilibrium and gave the lowest hornblende gabbronorite pressure for mineral cores; for this reason it is dashed in Figure 3b and excluded from further discussion.

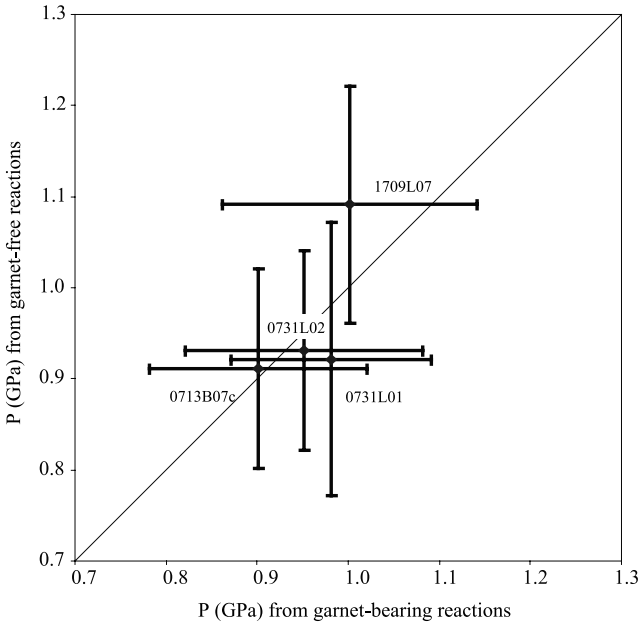

Figure 6. Pressures obtained from garnet hornblende gabbronorites using garnet-free equilibria differ from those obtained using garnet-bearing equilibria by <10%.

[18] Pressures for the Barnette Creek section span 0.53 to 0.91 GPa, but five of six samples occupy a narrower range of 0.53–0.72 GPa. The results are similar for the Tazlina section, with two samples spanning 0.59–0.62 GPa, and one outlier at 0.39 GPa. The pressures derived from hornblende gabbronorite mineral rims from Scarp Mountain and Bernard Mountain range from 0.93 to 1.24 GPa. This is essentially the same range as the pressures derived from garnet-bearing rocks from the same areas (0.83–1.22 GPa).

6. Calcsilicates

[19] Contact metamorphic rocks are a volumetrically minor portion of the arc. Metagabbros, quartzofeldspathic metasedimentary rocks, and calcsilicate rocks occur as kilometer- to meter-scale screens between plutons; calcsilicate assemblages are also developed in and around strongly deformed carbonate veins that cut the plutonic section of the arc and were then metamorphosed. P-T calculations for these rocks are shown in Table 5 and Figure 3c.

[20] Samples 2710B02a and 2714B03 are calcsilicate metasedimentary rocks intruded by igneous rocks. The mineral assemblages in these rocks are grossular-andradite garnet + diopside + plagioclase + calcite ± sphene + quartz ± scapolite. Samples 0713B05a, 1719P03b, 1804L01, 1804L03, 2720B01b are calcsilicates produced by metamorphism of calcite veins injected into mafic–intermediate igneous rock. Textural zones around the veins show that garnet was produced by reaction between igneous clinopyroxene and plagioclase fluxed by the introduced CO_2-rich fluid. The high-temperature mineral assemblages included grossular–andradite garnet + diopside + plagioclase + calcite ± sphene ± quartz; in some samples, rare symplectite intergrowths of calcite + quartz suggest that wollastonite was also present. Locally, particularly in the Klanelneechena Klippe, strong ductile deformation of these rocks produced disharmonic tight to isoclinal folds and garnet porphyroclasts within a calcite-rich matrix. These folds and garnets are cut by later calcite veins, suggesting a continuum of veining, deformation and reaction. The higher-grade mineral assemblages were strongly overprinted by a prehnite-pumpellyite facies alteration that produced chlorite from garnet; epidote, prehnite and pumpellyite from plagioclase; quartz + calcite from wollastonite; and datolite ($CaBSiO_4OH$) from wollastonite(?); and was accompanied by pervasive brittle deformation.

[21] Calculating pressures and temperatures for the calcsilicate rocks is tenuous for several reasons: (1) nearly all garnet and clinopyroxene grains have large calculated ferric iron components; (2) most plagioclase has been replaced by epidote, prehnite and pumpellyite; (3) almost all Mg was partitioned into clinopyroxene (Figure 2), rendering calculation of Fe-Mg exchange between garnet and clinopyroxene problematic; and (4) the presence of CO_2 introduces another variable. On the positive side, the absence of muscovite as an alteration product and the presence of <0.1 wt % Na_2O in some samples suggest that the plagioclase was anorthite. Moreover, the absence of hydrous phases suggests a high CO_2 activity.

[22] Sample 2710B02a is from a calcsilicate layer within amphibolite near Wolverine Creek. The presence of unaltered plagioclase means that pressure can be calculated with

Table 5. PT Conditions for Calc-Silicates[a]

Sample	T, °C	Method	P ± 1σ, GPa	Method	Cor
0713B05a	~950	GC	1.24 ± 0.65	g cpx	n/a
	941 ± 61	g cpx p q cc; aCO2 = 1	1.25 ± 0.14	g cpx p q cc; aCO2 = 1	−0.36
1719P03b	~800	GC	0.35–0.53 ± 0.23	GADS	n/a
1804L01	~800	GC	1.47 ± 1.35	g cpx	n/a
	791 ± 81	g cpx p q cc; aCO2 = 1	1.27 ± 0.15	g cpx p q cc; aCO2 = 1	−0.66
1804L03	~800	GC	1.09 ± 0.62	g cpx	n/a
	818 ± 79	g cpx p q cc; aCO2 = 1	1.37 ± 0.14	g cpx p q cc; aCO2 = 1	−0.60
2710B02a	907 ± 250	GC	1.00 ± 0.35	GADS	0.98
	876 ± 54	g cpx p q cc	0.96 ± 0.22	g cpx p q cc	0.69
2714B03	642 ± 180	g cpx p q cc	0.64 ± 0.27	g cpx	0.98
2720B01b	~650	GC	0.44–0.59 ± 0.17	GADS	n/a

[a]A "method" abbreviation indicates that a single reaction was used. GADS defined in text; GC, almandine–pyrope + diopside–hedenbergite equilibrium; and separate letters (e.g., "g h c p") indicate that all equilibria involving those minerals were used: b, biotite; c, clinopyroxene; cc, calcite; g, garnet; h, hornblende; m, muscovite; o, orthopyroxene; p, plagioclase; q, quartz; s, spinel. Cor, correlation coefficient between P and T uncertainties; n/a, not applicable.

Table 6. PT Conditions for Rocks Beneath the Klanelneechena Klippe[a]

Sample	T, °C	Method	P, GPa	Method	Cor
2718P10A	614 ± 102	GH	1.52 ± 0.57	GHPQ	0.69
2718P10A	598 ± 146	GH	1.18 ± 0.41	g h p q	0.93
2718P10C	494 ± 48	GH	1.21 ± 0.39	GHPQ	0.63
2718P10E	540 ± 65	GH	1.18 ± 0.59	GHPQ	0.66
2718P10E	618 ± 81	all	1.20 ± 0.21	g h p q m	0.89
2718P10I	492 ± 54	GH	1.16 ± 0.54	GHPQ	0.90
2718P10I	571 ± 79	all	1.16 ± 0.21	g h p q m	0.88

[a]A "method" abbreviation indicates that a single reaction was used. GH, pyrope–almandine + ferro-actinolite–tremolite equilibria; GHPQ, pyrope–almandine + ferro-actinolite–tremolite–tschermakite–pargasite + albite + quartz equilibria; and separate letters (e.g., "g h p q") indicate that all equilibria involving those minerals were used: g, garnet; h, hornblende; m, muscovite; p, plagioclase; q, quartz. Cor, correlation coefficient between P and T uncertainties.

the GADS net transfer reaction; intersection of this equilibrium with the garnet-clinopyroxene Fe-Mg exchange reaction gives P-T conditions of 1.00±0.35 GPa and 907 ± 250°C. The P-T intersection among all equilibria for this sample is 0.96 ± 0.22 GPa and 876 ± 54°C, and only for CO_2 activities $\geq$0.9.

[23] Two samples (1719P03b and 2720B01b) from deformed calcsilicate veins/layers within the Klanelneechena Klippe contain assemblages appropriate for GADS barometry, but the plagioclase is entirely altered to a mixture of pumpellyite and epidote. The absence of albite in the prehnite-pumpellyite alteration assemblages and the small amount of Na_2O in clinopyroxene suggests that the plagioclase was anorthite rich. Probable bounds to the anorthite content, based on plagioclase composition in nearby garnet gabbros, are 1.0 and 0.65. Garnet-clinopyroxene Fe-Mg exchange thermometry for 2720B01b gives temperatures of ~650°C and GADS barometry suggests pressures of 0.44–0.59 ± 0.17 GPa at this temperature for anorthite activities between 1.0 and 0.65. Likewise, garnet-clinopyroxene Fe-Mg exchange thermometry suggests temperatures of ~800°C for 1719P03b, similar to that inferred from nearby garnet gabbros (704–836°C); GADS barometry for this sample suggests pressures of 0.35 ± 0.19 GPa for a_{an} = 1 and 0.53 ± 0.23 for a_{an} = 0.65. In the presence of calcite, all equilibria for all phases other than plagioclase intersect at these same PT conditions only for CO_2 activities of ~1.

[24] Three samples (0713B05a, 1804L01, 1804L03) are centimeter-scale calcsilicate veins cutting gabbro on Scarp and Bernard Mountains. Plagioclase in these samples is altered to epidote + albite in modal proportions suggesting that the original plagioclase was ~An_{80}. Garnet-clinopyroxene Fe-Mg exchange thermometry suggests temperatures of ~800–950°C, the same temperatures inferred for nearby garnet gabbros. Equilibria involving only garnet and clinopyroxene, particularly the Ca-Tschermak component, are not influenced by the composition of plagioclase or the CO_2 activity. These equilibria suggest pressures of 1.24 ± 0.65 GPa (0713B05a), 1.47 ± 1.35 GPa (1804L01), and 1.09 ± 0.62 GPa (1804L03). Additional equilibria involving An_{80} plagioclase and calcite intersect at these PT conditions only for aCO_2 = 1 (e.g., reducing aCO_2 to 0.7 reduces the pressure by 0.3 GPa), and yield tighter constraints of 1.25 ± 0.14 GPa and 941 ± 61°C (0713B05a), 1.27 ± 0.15 GPa and 791 ± 81°C (1804L01), and 1.37 ± 0.14 GPa and 818 ± 79°C (1804L03).

[25] A calcsilicate (2714B03) collected from John Creek in the northern Talkeetna Mountains contains scapolite and An_{37} plagioclase. Equilibria that are independent of aCO_2 and involve garnet, clinopyroxene, plagioclase and quartz, intersect at 0.64 ± 0.27 GPa and 642 ± 180°C.

[26] In summary, the calcsilicate from Wolverine suggests that the Moho at Wolverine was at the same pressure (0.96 GPa) as the Scarp and Bernard garnet gabbros (0.8–1.2 GPa). The Klanelneechena Klippe calcsilicates indicate pressures (0.53–0.59 GPa) at minimum probable anorthite contents that overlap, within uncertainty, pressures calculated for nearby garnet gabbros (0.69–0.77 GPa). The calcsilicates from Scarp and Bernard Mountains gave pressures (1.25–1.37 GPa) that are rather uncertain, but similar to those inferred for the garnet gabbros from Scarp Mountain (0.8–1.2 GPa). The general correspondence between the temperatures inferred for the calcsilicate rocks and nearby metamafic rocks suggests that the calcsilicate assemblages grew during the development of the arc, before the arc had cooled more than 100°C.

7. Metamorphic Rocks in the McHugh Complex

[27] Metamorphic rocks were discovered in outcrops of volcaniclastic metasediments, probably belonging to the McHugh Complex, structurally beneath the Klanelneechena Klippe and as locally derived float in moraines along the eastern edge of the klippe. Garnet was found only in float, and pressures and temperatures were determined from these garnet-bearing samples. However, samples from outcrops are otherwise mineralogically and compositionally similar to the garnet-bearing samples. These rocks all contain a strong amphibolite-facies fabric defined by garnet and albite porphyroblasts and aligned hornblende and plagioclase; that these minerals were coeval is suggested by their similar grain size, lack of grain boundary reactions, and (in the case of garnet and albite) similar inclusion trails. They are overprinted by a greenschist(?)-facies fabric defined by albite + quartz veins and chlorite-filled strain shadows around some garnets. High P/T ratios are qualitatively indicated by the presence of albite, the absence of biotite, and >3 wt % Na_2O in magnesiohornblende. The minerals in these samples are compositionally different from minerals in all of the rocks discussed so far, suggesting that these rocks are unrelated to the arc. Garnets show strong prograde zoning with decreasing Mn, increasing Ca, and increasing Mg #. We calculated pressures and temperatures using garnet rims. Hornblende and muscovite show minor patchy zoning and the uncertainties in the values in Table 6 reflect this. All samples yield equilibration conditions of ~500–600°C and ~1.2 GPa (Figure 3d).

8. Al-in-Hornblende Barometry

[28] Intermediate to felsic plutonic rocks are common at midcrustal depths in the arc section, and a minor subset of these evolved plutons contain the mineral assemblage required for Al-in-hornblende barometry (i.e., hornblende + biotite + plagioclase + quartz + orthoclase + sphene + ilmenite/magnetite [*Johnson and Rutherford*, 1989;

Table 7. Al-in-Hornblende Barometry and Hornblende-Plagioclase Thermometry[a]

Sample	*Johnson and Rutherford* [1989], GPa	*Schmidt* [1992], GPa	*Blundy and Holland* [1990], °C
0719T04	0.06 ± 0.05	0.15 ± 0.07	647 ± 77
0720G02	0.1 ± 0.05	0.27 ± 0.08	692 ± 75
1728M05a	0.03 ± 0.05	0.13 ± 0.06	719 ± 75
2714M02	0.14 ± 0.05	0.22 ± 0.06	682 ± 75

[a]Uncertainties are 1σ and reflect calibration uncertainty and variability in mineral composition, added in quadrature.

Schmidt, 1992]). Four samples containing this igneous mineral assemblage were analyzed for Al-in-hornblende barometry (Table 7 and Figure 3b). The samples are weakly deformed and show weak (sub)greenschist-facies alteration. Plagioclase typically is zoned from andesine to oligoclase; the amphiboles are all magnesiohornblende, with +9 to −14% core-rim zoning in Al. The pressures calculated from mineral rim compositions lie at or below the minimum pressures in experiments used to calibrate the barometer (e.g., 0.25 GPa in the case of *Schmidt* [1992]); but this casts only minor doubt on their veracity because of the linear nature of the ∂Al/∂P dependence. Temperatures determined from the rim compositions of coexisting hornblende and plagioclase [*Blundy and Holland*, 1992] are mostly within the range of the experimental temperatures imposed by *Schmidt* [1992] (655–700°C) but are colder than those used by *Johnson and Rutherford* [1989]. Because the Al content of hornblende in this assemblage is a function of P and T, the pressures derived from the *Schmidt* [1992] calibration (0.13 to 0.27 GPa) are therefore preferred.

9. Discussion

9.1. Pressures Within the Gabbronorite Section

[29] Most of the P-T data for the arc gabbronorites come from the Tazlina and Barnette sections and have straightforward interpretations. The pressures calculated for the Barnette sample rims, with one exception, give a narrow pressure range (0.53–0.72 GPa). Because these samples crop out within <1000 m of each other, this range of pressures may simply be scatter about a single number, with a weighted mean at the 95% C.I. of 0.64 ± 0.15 GPa. Alternatively, they could represent real variation related to (re)crystallization of gabbronorites at different times when the arc had different thicknesses; these two different scenarios lead to quite distinct conclusions about the composition of the arc, as discussed below. The one slightly higher-pressure outlier from Barnette might be a late stage metamorphic overgrowth, as the pressure determined from the mineral cores for that sample overlaps the pressures determined for the mineral rims of the other samples. The same issue pertains to the Tazlina section (except that there the outlier gives slightly lower pressure), such that the restricted pressure range for the mineral rims (0.59–0.62 GPa) may reflect scatter about a weighted mean pressure of 0.60 ± 0.39 GPa (95% C.I.) or could record different stages of (re)crystallization at different arc thicknesses.

9.2. Depth of the Moho

[30] Interpreting the pressures from the gabbronorites in the supra-Moho Scarp Mountain section is not straightforward. Our inability to recover peak pressures and temperatures notwithstanding, there appears to be a systematic difference in pressure between the garnet-bearing and garnet-free samples from Scarp Mountain; moreover, contrary to expectations, the samples yielding pressures greater than 1 GPa do not contain garnet (Figure 2), whereas the garnet-bearing samples give pressures less than 1 GPa (regardless of whether garnet is included in the equilibria used to calculate pressure, implying that the calculated pressures are not being held hostage by an inaccurate activity model). Moreover, two garnet-bearing and three garnet-free rocks from Scarp Mountain show only minor differences in bulk composition (Table 2), and all have similar garnet-in reaction positions at an f_{O2} of NNO + 2 (see *Behn and Kelemen*'s [2006] Figure 3 for P-T-f_{O2} systematics) as calculated by Perple_X [*Connolly*, 1990] (shaded area in Figure 3). If, however, the relative uncertainties among the pressures derived from the hornblende gabbronorites at Scarp Mountain are equivalent to (or slightly less than) the uncertainties in Table 4, the pressures form a single population with a weighted mean of 1.00 ± 0.11 GPa, identical to that inferred for samples from the same area using garnet-bearing equilibria.

[31] This explanation still leaves another issue: Why, for a small range in bulk compositions and P-T conditions, do some samples contain garnet and others not? Does this reflect (1) uncertainty in the thermobarometry, (2) kinetic factors, (3) variations in oxygen fugacity, or (4) actual changes in the thickness of the arc? The first two possibilities imply that the garnet-free samples crystallized at temperatures above the garnet-in reaction and then cooled without forming garnet. The most probable influences on kinetics are deformation and the activity of H_2O; the presence of hornblende in most samples, however, suggests a relatively constant H_2O fugacity. Using Perple_X [*Connolly*, 1990], *Behn and Kelemen* [2006, Figure 3 and associated text] found that equilibrium mineral assemblages in Talkeetna hornblende-oxide-gabbronorites depend critically on oxygen fugacity. At 0.9–1.2 GPa and 700–1100°C, garnet-free assemblages are predicted in Talkeetna gabbronorite bulk compositions for f_{O2} greater than nickel-nickel oxide (NNO) + 2, whereas garnet-bearing assemblages are predicted at lower oxygen fugacity. Thus, if oxygen fugacity near the Talkeetna Moho was variable during peak metamorphism, with local values below and above the NNO buffer, this could explain the presence or absence of garnet in otherwise similar bulk compositions.

[32] Considering the fourth possibility, if the ~0.2 GPa variation in pressure is the result of thickening or thinning of the arc, ~7 km of thickness change is required. If it was thickening, the ~1.0 GPa garnet-bearing rocks must have formed early and then been carried down to ~1.2 GPa where the garnet-free rocks formed. All the rocks must then have cooled, recording low temperatures within the garnet stability field, though some samples passed through these conditions without forming garnet. If the 0.2 GPa variation reflects 7 km of thinning, the ~1.2 GPa garnet-free rocks must have formed and then been carried upward during thinning, at which time the ~1.0 GPa garnet-bearing rocks formed. Both the thickening and thinning hypotheses are compatible with the observed core–rim zoning, which implies cooling.

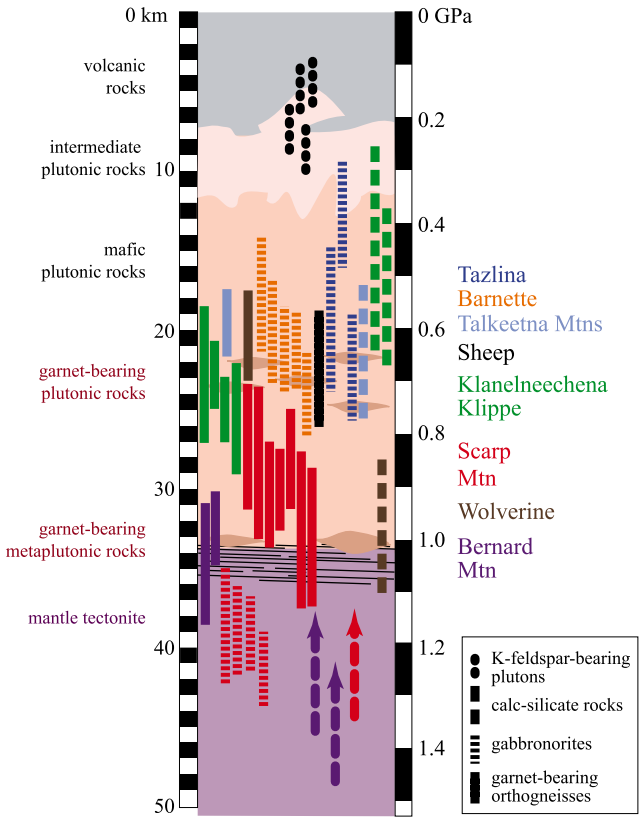

Figure 7. A pseudostratigraphic column for the Talkeetna arc reconstructed on the basis of thermobarometry presented in this study: K-feldspar bearing plutons crystallized at 5–9 km, most hornblende gabbronorites crystallized at 17–24 km, Klanelneechena Klippe crystallized at 22–24 km, and garnet gabbros crystallized at the base of the arc at ~30. Uncertainties are $\pm 0.5\sigma$ for clarity. Arrowheads on three highest pressures indicate that these are maxima; real pressures were lower and depend on indeterminate a_{CO2}.

[33] A number of other aspects of the arc geology suggest thickening: (1) rafts of amphibolite derived from arc lava and metasediment locally form the host rock to intrusions, (2) the formation of two-pyroxene + spinel assemblages from olivine-plagioclase websterite is compatible with increasing pressure (Figure 4), (3) the garnet-bearing rocks in the Klanelneechena klippe may be restites from melting of intermediate volcanic rocks [*Kelemen et al.*, 2003a], and (4) if the 7-km-thick volcanic section was intruded by tonalites and quartz diorites at depths as shallow as 5 km, the volcanic section may have continued to thicken after the intrusions had solidified.

9.3. Significance of the High-Pressure Rocks in the McHugh Complex

[34] The high-pressure garnet amphibolites in the McHugh Complex formed at pressures similar to the base of the arc exposed on Scarp Mountain, and at pressures ~0.5 GPa greater than the immediately overlying Klanelneechena Klippe portion of the arc; they record temperatures significantly cooler than any part of the arc section. They crop out on the SW side of the Klanelneechena Klippe, along strike of the belt of Iceberg Lake schist mapped within the McHugh Complex by *Winkler et al.* [1981]. Good constraints on the P-T conditions of the Iceberg Lake schist, a lawsonite-garnet blueschist, cannot yet be derived, but reported mineral compositions and parageneses [*Sisson and Onstott*, 1986] indicate lower temperatures than the garnet amphibolites. Because the Iceberg Lake schist and the garnet amphibolite are the only two high-pressure rocks in the area, we provisionally assume that they are related and adopt the phengite $^{40}Ar/^{39}Ar$ age of 187.0 ± 1.5 Ma for the Iceberg Lake schist (*Sisson and Onstott* [1986], corrected using the work by *Renne et al.* [1998]) as the approximate age for the garnet amphibolites. This tentative age assignment implies that the garnet amphibolites formed at the same time as the Talkeetna arc [*Rioux et al.*, 2007a; B. R. Hacker et al., Cooling history of the Talkeetna intra-oceanic arc of Alaska: $^{40}Ar/^{39}Ar$ and U-Th/He dating, manuscript in preparation, 2008] and must have subsequently been faulted into their present location.

9.4. Reconstructing the Talkeetna Arc

[35] The data bearing on reconstruction of the Talkeetna arc section are thus as follows: (1) the volcanic section is estimated from stratigraphy to be 7 km thick [*Clift et al.*, 2005a]; (2) the tonalites and quartz diorites we analyzed crystallized at 0.13–0.27 GPa; (3) the hornblende gabbronorites of the Tazlina section formed at ~0.59–0.62 GPa; (4) the hornblende gabbronorites of the Barnette section formed at ~0.53–0.72 GPa; (5) the garnet diorites in the Klanelneechena Klippe crystallized at ~0.73 GPa; and (6) the garnet gabbros, spinel-rich pyroxenites and orthogneisses, and hornblende gabbronorites at the base of the arc in the Scarp and Barnard areas recrystallized at ~0.9–1.2 GPa. To convert these pressures to depth, we assume a density for the volcanic section of 2.9 g/cm^3 and a density for the plutonic section of 3.1 g/cm^3 [*Behn and Kelemen*, 2006]. This assumption yields crystallization depths of 5–9 km for the granodiorites, ~19–22 km for the Tazlina gabbronorites, ~17–24 km for the Barnette gabbronorites, ~24 km for the Klanelneechena Klippe garnet diorites, and 30–35 km for the base of the section (Figure 7). We identified no samples that might constitute older basement into which the arc intruded.

[36] Thus, at some time the Talkeetna arc consisted of a 7-km-thick volcanic section overlying a ~23- to 28-km-thick plutonic section, or a volcanic:plutonic ratio of 1:3 to 1:4. There are, however, at least two important aspects of the arc that we cannot constrain with the present data set.

[37] 1. What are the age relationships among the various pressures? Are the recorded pressures coeval throughout the section or do they span a significant time interval, say 10 Ma? The answer to this question affects how one reconstructs the arc. If the pressures are coeval, the present column provides at least a snapshot of the arc constitution at one time; if not, the present distribution of rocks may differ substantially from the constitution of the arc at any given time during its evolution.

[38] 2. Do the ranges in pressure inferred for the individual Barnette, Tazlina, Scarp and Bernard sections indicate changes in pressure over time? As noted above, most of the

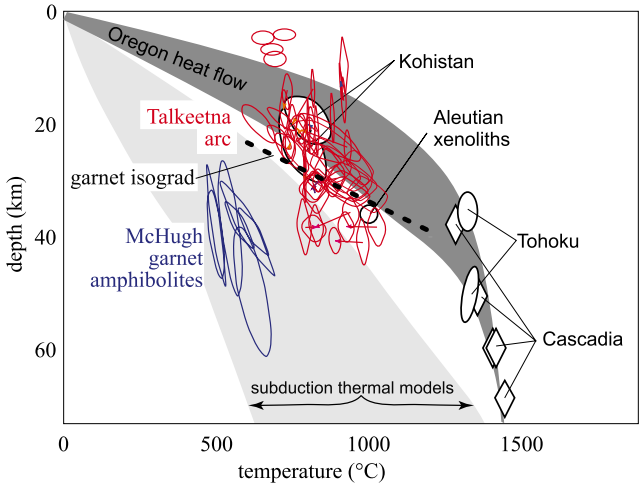

Figure 8. The bulk of the Talkeetna arc section records a thermal gradient (compare Figure 3) similar to that inferred for arcs worldwide, but the deepest part of the arc records cooler temperatures than inferred for active arcs. P-T conditions inferred for McHugh Complex are similar to relatively cold subduction zones. See *Kelemen et al.* [2003b] for explanation of data from worldwide arcs.

Barnette samples define a pressure range of 0.53–0.72 GPa. If this is a true range in pressure resulting from diachronous recrystallization, the Barnette section defines the composition of the ~17–24 km depth range of the arc over some time period. If instead these data reflect scatter about a mean pressure of 0.64 GPa, the Barnette section defines only the composition of a <1-km-thick section at ~21 km. The same uncertainties apply to the Tazlina, Scarp, and Bernard sections.

9.5. Implications for Thermal Gradients in Arcs

[39] *Kelemen et al.* [2003b] used a variety of data from metamorphic rocks, volcanic rock compositions, heat flow, and thermal models to infer a typical range of thermal gradients in arcs (Figure 8). The thermal conditions we infer for the bulk of the Talkeetna arc are compatible with, but fall on the colder side, of that range of thermal gradients. The highest-pressure samples from the base of the Talkeetna arc show hundreds of degrees of deviation from the inferred range of typical arc gradients, and, in particular, are incompatible with temperature estimates for melt-mantle equilibration derived from the modern Tohoku [*Tatsumi et al.*, 1983] and Cascadia [*Elkins Tanton et al.*, 2001] arcs. Moreover, the Talkeetna garnet-bearing rocks are not compatible with the warmest thermal gradients inferred by Kelemen et al., as garnet is not stable at pressures less than the "garnet isograd" in Figure 8. This is a further indication that the base of the Talkeetna arc may not have formed at the P-T conditions currently preserved in the rocks and may have been hotter while the arc was active.

9.6. Deformation of the Talkeetna Arc

[40] The current 5–7 km structural thickness of the plutonic section of the arc represents only ~15–30% of the original 23–28 km thickness. This observation raises the question of how and when this thinning occurred, both of which have implications for reconstructing the arc section and for the tectonic development of the arc. If the thinning occurred via pure shear, as a hypothetical end-member, the present crustal section preserves all compositions and proportions, albeit in a thinner version. Alternatively, if the thinning was accomplished by a host of faults or shear zones of arbitrary location, orientation, and strain, the present crustal section (other than those portions for which pressures have been determined) need not correspond to any former constitution of the arc.

[41] It is entirely possible that the thinning occurred while the arc was active, during the subduction erosion that has been inferred for the Talkeetna arc [*Clift et al.*, 2005b]; it is possible, for example, that ~0.6 GPa gabbronorites were intruded just above the former 1 GPa Moho section following large-scale thinning. The late Mesozoic deformation along the Border Ranges fault system (N-S shortening and vertical thickening [*Pavlis*, 1982]) was of the wrong sense to thin the arc unless the arc section was more steeply dipping then than now. This was, however, followed by Paleocene N-S extension and vertical thinning that unroofed the arc [*Little and Naeser*, 1989]. If this deformation thinned the arc, it was apparently minimal because the current outcrop width of the plutonic section nowhere exceeds 10–15 km. A solution may be found in the Eocene dextral wrenching along the Border Ranges fault system; this deformation produced shear strains of 2–3 from WSW-ENE extension and NNW-SSE shortening [*Little and Naeser*, 1989; T. Little, personal communication, 2006]. If the Talkeetna arc had been favorably oriented, this deformation could have been largely responsible for the observed thinning.

9.7. Implications for Intraoceanic Arcs and Crustal Genesis

[42] The crustal section that we infer for the Talkeetna arc, including the uncertainties previously discussed, can be used to determine the bulk composition and physical properties for the arc crust [*Behn and Kelemen*, 2006]. The major uncertainties from thermobarometry are: do the rocks in an individual section (e.g., Barnette Creek) define the composition of (1) a multikilometer depth range or (2) a <1-km-thick section at a specific depth? And, was the plutonic section (1) thinned by pure shear, such that the lithologies exposed are representative of what was lost, or

Table 8a. Average Normalized Compositions of Rock Types in the Talkeetna Arc[a]

	Lava	Felsic Pluton	Mafic Pluton	Klanel-neechena	Scarp Mountain	Pyroxenite
SiO_2	59.64	68.54	47.86	51.6	43.78	49.95
TiO_2	0.86	0.5	0.66	0.89	0.82	0.07
Al_2O_3	16.53	15.19	19	18.92	21.76	3.42
FeO*	7.78	4.06	9.94	10.3	9.76	8.31
MnO	0.19	0.11	0.18	0.21	0.12	0.17
MgO	3.57	1.67	7.78	4.89	8.28	27.95
CaO	6.3	4.66	12.53	10.41	13.9	9.88
Na_2O	3.82	4.38	1.82	2.51	1.3	0.22
K_2O	1.03	0.76	0.16	0.13	0.06	0.02
P_2O_5	0.18	0.13	0.08	0.14	0.1	0.01

[a]Unit is wt %.

Table 8b. Thicknesses of Rocks in Reconstructed Columns of the Talkeetna Arc[a]

Model (Figure 9)	Lava	Felsic Pluton	Mafic Pluton	Klanel-neechena	Scarp Mountain	Pyroxenite	Sum
1a	5	8	10	3	9	0.2	35.2
$1a^{pxnt}$	5	8	10	3	9	10	45
2a	5	8	10	4	7	0.2	34.2
$2a^{pxnt}$	5	8	10	4	7	10	44
1b	5	4	15	1	10	0.2	35.2
$1b^{pxnt}$	5	4	15	1	10	10	45
2b	5	4	14	1	10	0.2	34.2
$2b^{pxnt}$	5	14	4	7	4	10	44
1c	5	13	5	4	8	0.2	35.2
$1c^{pxnt}$	5	13	5	4	8	10	45
2c	5	14	4	7	4	0.2	34.2
$2c^{pxnt}$	5	14	4	7	4	10	44

[a]Unit is km. Superscript pxnt denotes reconstructions with 10-km-thick pyroxenite layers to bring the Mg # of the arc to ~0.7, consistent with Fe/Mg equilibrium with residual mantle peridotite.

(2) thinned heterogeneously, such that the composition of the missing section is unknown? Additional uncertainties are that the felsic plutonic rocks and lower crustal rocks are different in different places, and a substantial section of pyroxenite may be missing from the base of the plutonic section. For example, the garnet-bearing rocks in the Klanelneechena Klippe are quite different from those at the base of the arc, and yet the entire intervening section could have contained garnet.

[43] A range of bulk compositions (Tables 8a–8c) can be calculated using the methodology outlined in Figure 9. Calculations for pure shear thinning are simple and yield arc SiO_2 contents of 53–54 wt %, with the 1 wt % range in SiO_2 a function of whether the pyroxenite at the top of the mantle is considered to be 0.2 km thick, as in the preserved Bernard-Scarp section, or 10 km thick, as is required to bring the crustal bulk compositions to an Mg # of ~0.7, consistent with Fe/Mg equilibrium with residual mantle peridotite. The most felsic arc composition, 56–58 wt % SiO_2, is obtained from section 2c, in which each of the missing depth intervals is replaced with the overlying rock type. Conversely, the most mafic arc composition, 51 wt % SiO_2, is obtained from section 1b, in which each of the missing depth intervals is replaced with the underlying rock type. Most of the other major elements do not vary greatly among the various models, except for Al_2O_3, which decreases by ~0.3 wt % for each km of added pyroxenite, and MgO, which increases by ~0.5 wt % for each km of added pyroxenite.

9.8. Comparison With Other Arc Sections

[44] There are two other relatively well investigated arcs with garnet-bearing basal crustal sections. The Jijal Complex at the base of the Kohistan Arc includes garnet granulites formed at 700–950°C and >1 GPa [*Yamamoto and Yoshino*, 1998; *Yoshino and Okudaira*, 2004]. Whether these garnet granulites formed during igneous cooling [*Ringuette et al.*, 1999], postmagmatic heating and compression [*Yoshino et al.*, 1998], or dehydration melting of hornblende [*Garrido et al.*, 2006] is controversial. The Fiordland, New Zealand lower crustal contains garnet granulite formed in hornblende gabbronorite at >750°C and 1.4 GPa during either in situ dehydration melting [*Blattner and Black*, 1980], fluid migration [*Blattner*, 2005] or melt migration [*Clarke et al.*, 2000; *Daczko et al.*, 2001; *Clarke et al.*, 2005]. The garnet granulites in Kohistan form irregular veins and lenses within hornblende gabbronorite, similar to the basal section at Talkeetna, whereas in the least deformed sections in Fiordland the granulite developed on the margins of rather rectilinear anorthositic veins. Both Kohistan and Fiordland have much thicker preserved garnet-bearing sections than Talkeetna, at 6 km and 10 km, respectively, but, as noted above, the reconstructed section permits that the Talkeetna arc once had a garnet-bearing section of comparable thickness.

10. Conclusions

[45] Thermobarometry of the Talkeetna arc reveals that tonalites and quartz diorites intruded at ~5–9 km depth into a 7-km-thick volcanic section. Hornblende gabbronorite sections that were investigated crystallized at ~17–24 km. Diorites with igneous garnet formed at ~24–26 km; and garnet granulites at the base of the arc recrystallized at ~35 km depth. Temperatures at the base of the arc were in excess of 900°C, comparable to cooler arcs worldwide. Several textural and outcrop-scale features indicate synmagmatic thickening of the arc, but no arc basement was

Table 8c. Compositions of Reconstructed Columns of the Talkeetna Arc[a]

Model (Figure 9)	SiO_2	TiO_2	Al_2O_3	FeO*	MnO	MgO	CaO	Na_2O	K_2O	P_2O_5
1a	53.5	0.7	18.4	8.3	0.15	5.8	10.0	2.6	0.4	0.12
$1a^{pxnt}$	52.7	0.6	15.1	8.3	0.16	10.6	10.0	2.1	0.3	0.09
2a	54.0	0.7	18.2	8.2	0.16	5.6	9.8	2.7	0.4	0.12
$2a^{pxnt}$	53.1	0.6	14.9	8.3	0.16	10.6	9.8	2.1	0.3	0.09
1b	50.8	0.7	18.9	8.9	0.16	6.7	11.1	2.3	0.3	0.11
$1b^{pxnt}$	50.6	0.6	15.5	8.8	0.16	11.3	10.8	1.8	0.3	0.08
2b	50.9	0.7	18.9	8.9	0.16	6.6	11.0	2.3	0.3	0.11
$2b^{pxnt}$	56.5	0.5	14.2	7.5	0.16	9.5	8.5	2.6	0.4	0.10
1c	56.7	0.7	17.8	7.5	0.14	4.8	8.8	3.0	0.5	0.12
$1c^{pxnt}$	55.2	0.6	14.6	7.6	0.15	9.9	9.0	2.4	0.4	0.10
2c	58.3	0.7	17.3	7.3	0.15	4.2	8.1	3.2	0.5	0.13
$2c^{pxnt}$	56.5	0.6	14.2	7.5	0.16	9.5	8.5	2.6	0.4	0.10

[a]Superscript pxnt denotes reconstructions with 10-km-thick pyroxenite layers to bring the Mg # of the arc to ~0.7, consistent with Fe/Mg equilibrium with residual mantle peridotite.

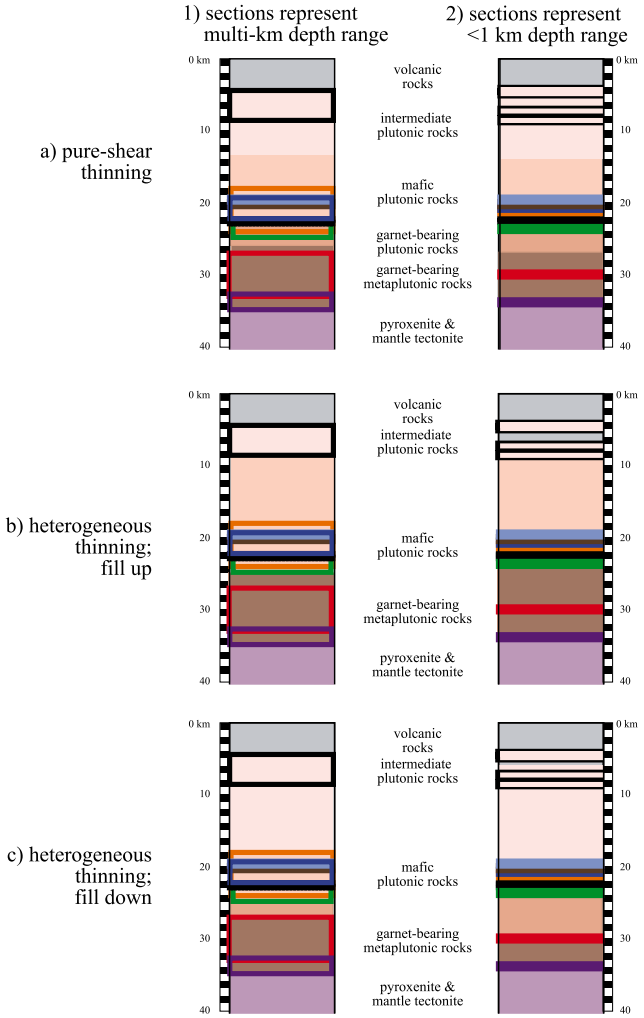

Figure 9. A range of possible reconstructed sections for the Talkeetna arc, based on calculated pressures (excluding calcsilicates) and exposed rock types; see Tables 8a–8c for the resultant bulk compositions, which vary from 51 to 58% SiO_2. (left) Assumption 1 is that the range of pressures determined from each of the study areas (e.g., Barnette Creek) represents a real range in pressure. (right) Assumption 2 is that the same range represents analytical scatter about a mean pressure (see text). Assumption 1 means that much of the arc composition is known, whereas assumption 2 means that much of the composition is unknown. (a) Arc thinning was accomplished by pure shear. (b) Thinning was accomplished by heterogeneous faulting and that missing sections are composed of underlying rocks, resulting in the most mafic possible solution. (c) Heterogeneous faulting and that missing sections are composed of overlying rocks, resulting in the most felsic possible solution. See Figure 7 for explanation of colors.

identified. Only ~15–30% of the original thickness of the plutonic section survives today, and whether the missing sections were identical or different in composition to the exposed portions is unknown. Given this ambiguity, the bulk composition of the Talkeetna arc is only loosely constrained to ~51–58 wt % SiO_2.

[46] **Acknowledgments.** Funded by NSF EAR-9910899. William D. Carlson of the University of Texas, Austin, completed the garnet diffusion modeling. George Bergantz and Geoff Clarke provided constructive reviews.

References

Andersen, D. J., D. H. Lindsley, and P. M. Davidson (1993), QUILF; a Pascal program to assess equilibria among Fe-Mg-Mn-Ti oxides, pyroxenes, olivine, and quartz, *Comput. Geosci.*, *19*, 1333–1350.

Behn, M. D., and P. B. Kelemen (2006), Stability of arc lower crust: Insights from the Talkeetna arc section, south central Alaska, and the seismic structure of modern arcs, *J. Geophys. Res.*, *111*, B11207, doi:10.1029/2006JB004327.

Berman, R. G., and T. H. Brown (1992), Thermobarometry with estimation of equilibration state [TWEEQU]; a software package for IBM or compatible personal computers, *Open File Rep. Geol. Surv. Can.*, *2534*.

Blattner, P. (2005), Transport of low-aH2O dehydration products to melt sites via reaction-zone networks, Milford Sound, New Zealand, *J. Metamorph. Geol.*, *23*, 569–578.

Blattner, P., and P. M. Black (1980), Apatite and scapolite as petrogenetic indicators in granolites of Milford Sound, New Zealand, *Contrib. Mineral. Petrol.*, *74*, 339–348.

Blundy, J. D., and T. J. B. Holland (1990), Calcic amphibole equilibria and a new amphibole-plagioclase geothermometer, *Contrib. Mineral. Petrol.*, *104*, 208–224.

Blundy, J. D., and T. J. B. Holland (1992), Calcic amphibole equilibria and a new amphibole–plagioclase geothermometer: Reply to the comments of Hammarstrom and Zen and Rutherford and Johnson, *Contrib. Mineral. Petrol.*, *111*, 269–272.

Burns, L. E. (1985), The Border Ranges ultramafic and mafic complex, south-central Alaska: Cumulate fractionates of island arc volcanics, *Can. J. Earth Sci.*, *22*, 1029–1038.

Carlson, W. D. (2006), Rates of Fe, Mg, Mn, and Ca diffusion in garnet, *Am. Mineral.*, *91*, 1–11.

Clarke, G. L., K. A. Klepeis, and N. R. Daczko (2000), Cretaceous high-P granulites at Milford Sound, New Zealand; metamorphic history and emplacement in a convergent margin setting, *J. Metamorph. Geol.*, *18*(4), 359–374.

Clarke, G. L., N. R. Daczko, K. A. Klepeis, and T. Rushmer (2005), Roles for fluid and/or melt advection in forming high-P mafic migmatites, Fiordland, New Zealand, *J. Metamorph. Geol.*, *23*(7), 557–567.

Clift, P. D., A. E. Draut, P. B. Kelemen, J. Blusztajn, and A. Greene (2005a), Stratigraphic and geochemical evolution of an oceanic arc upper crustal section: The Jurassic Talkeetna Volcanic Formation, south-central Alaska, *Geol. Soc. Am. Bull.*, *117*, 902–925.

Clift, P. D., T. Pavlis, S. M. DeBari, A. E. Draut, M. Rioux, and P. B. Kelemen (2005b), Subduction erosion of the Jurassic Talkeetna-Bonanza Arc and the Mesozoic accretionary tectonics of western North America, *Geology*, *11*, 881–884.

Connolly, J. A. D. (1990), Multivariable phase diagrams an algorithm based on generalized thermodynamics, *Am. J. Sci.*, *290*, 666–718.

Daczko, N. R., G. L. Clarke, and K. A. Klepeis (2001), Transformation of two-pyroxene hornblende granulite to garnet granulite involving simultaneous melting and fracturing of the lower crust, Fiordland, New Zealand, *J. Metamorph. Geol.*, *19*(5), 547–560.

DeBari, S. M., and R. G. Coleman (1989), Examination of the deep levels of an island arc: evidence from the Tonsina ultramafic-mafic assemblage, Tonsina, Alaska, *J. Geophys. Res.*, *94*, 4373–4391.

de Capitani, C., and T. H. Brown (1987), The computation of chemical equilibrium in complex systems containing non-ideal solutions, *Geochim. Cosmochim. Acta*, *51*, 2639–2652.

Elkins Tanton, L. T., T. L. Grove, and J. Donnelly-Nolan (2001), Hot, shallow mantle melting under the Cascades volcanic arc, *Geology*, *29*, 631–634.

Garrido, C. J., J.-L. Bodinier, J.-P. Burg, G. Zeilinger, S. S. Hussain, H. Dawood, M. N. Chaudhry, and F. Gervilla (2006), Petrogenesis of mafic garnet granulite in the lower crust of the Kohistan Paleo-arc complex (northern Pakistan): Implications for intra-crustal differentiation of island arcs and generation of continental crust, *J. Petrol.*, *47*, 1873–1914.

Greene, A. R., S. M. DeBari, P. B. Kelemen, J. Blusztajn, and P. D. Clift (2006), A detailed geochemical study of island arc crust: The Talkeetna Arc section, south-central Alaska, *J. Petrol.*, *47*, 1051–1093.

Holland, T. J. B. (1990), Activities in omphacitic solid solutions: an application of Landau theory to mixtures, *Contrib. Mineral. Petrol.*, *105*, 446–453.

Holland, T. J. B., and R. Powell (1998), An internally consistent thermodynamic data set for phases of petrological interest, *J. Metamorph. Geol.*, *16*, 309–343.

Johnson, M. C., and M. J. Rutherford (1989), Experimental calibration of the aluminum-in-hornblende barometer with application to Long Valley caldera (California) volcanic rocks, *Geology*, *17*, 837–841.

Kelemen, P. B., K. Hanghøj, and A. Greene (2003a), One view of the geochemistry of subduction-related magmatic arcs, with an emphasis on primitive andesite and lower crust, in *Treatise on Geochemistry*, vol.3, *The Crust*, edited by R. L. Rudnick, pp.593–659, Elsevier, Oxford, U.K.

Kelemen, P. B., E. M. Parmentier, J. Rilling, L. Mehl, and B. R. Hacker (2003b), Thermal structure due to solid-state flow in the mantle wedge beneath arcs, in *Inside the Subduction Factory*, *Geophys. Monogr. Ser.*, vol. 138, edited by J. Eiler, pp. 293–311, AGU, Washington, D. C.

Liermann, H. P., and J. Ganguly (2003), Fe^{2+}-Mg fractionation between orthopyroxene and spinel; experimental calibration in the system FeO-MgO-Al_2O_3-Cr_2O_3-SiO_2, and applications, *Contrib. Mineral. Petrol.*, *145*(2), 217–227.

Little, T., and C. W. Naeser (1989), Tertiary tectonics of the Border Ranges Fault System, Chugach Mountains, Alaska: Deformation and uplift in a forearc setting, *J. Geophys. Res.*, *94*, 4333–4359.

Mehl, L., B. R. Hacker, G. Hirth, and P. B. Kelemen (2003), Arc-parallel flow within the mantle wedge: Evidence from the accreted Talkeetna arc, south central Alaska, *J. Geophys. Res.*, *108*(B8), 2375, doi:10.1029/2002JB002233.

Miller, C., A. Zanetti, M. Thöni, and J. Konzett (2007), Eclogitisation of gabbroic rocks: Redistribution of trace elements and Zr in rutile thermometry in an Eo-Alpine subduction zone (Eastern Alps), *Chem. Geol.*, *239*, 96–123.

Pavlis, T. L. (1982), Origin and age of the Border Ranges Fault of southern Alaska and its bearing on the late Mesozoic tectonic evolution of Alaska, *Tectonics*, *1*, 343–368.

Pavlis, T. L., and S. M. Roeske (2007), The Border Ranges fault system, southern Alaska, in *Tectonic Growth of a Collisional Continental Margin: Crustal Evolution of Southern Alaska*, edited by K. D. Ridgway et al., *Spec. Pap. Geol. Soc. Am.*, *431*, 95–128, doi:10.1130/2007.2431(05).

Plafker, G., W. J. Nokleberg, and J. S. Lull (1989), Bedrock geology and tectonic evolution of the Wrangellia, Peninsular, and Chugach terranes along the Trans-Alaska Crustal Transect in the Chugach Mountains and southern Copper River basin, Alaska, *J. Geophys. Res.*, *94*, 4255–4295.

Powell, R., and T. J. B. Holland (1988), An internally consistent dataset with uncertainties and correlations: 3. Applications to geobarometry, worked examples and a computer program, *J. Metamorph. Geol.*, *6*, 173–204.

Renne, P. R., C. C. Swisher, A. L. Deino, D. B. Karner, T. L. Owens, and D. J. DePaolo (1998), Intercalibration of standards, absolute ages and uncertainties in $^{40}Ar/^{39}Ar$ dating, *Chem. Geol.*, *145*, 117–152.

Ringuette, L., J. Martignole, and B. F. Windley (1999), Magmatic crystallization, isobaric cooling, and decompression of the garnet-bearing assemblages of the Jijal Sequence (Kohistan Terrane, western Himalayas), *Geology*, *27*(2), 139–142.

Rioux, M., B. R. Hacker, J. M. Mattinson, P. Kelemen, T. Plank, and P. Reiners (2003), The evolution of silicic magmatism in the accreted Talkeetna arc, south-central Alaska, *Eos Trans. AGU*, *84*(46), Fall Meet. Suppl., Abstract V31C-0949.

Rioux, M., B. R. Hacker, J. Mattinson, P. B. Kelemen, J. Blusztajn, and G. Gehrels (2007), The magmatic development of an intra-oceanic arc: High-precision U-Pb zircon and whole-rock isotopic analyses from the accreted Talkeetna arc, south-central Alaska, *Geol. Soc. Am. Bull.*, *119*(9–10), 1168–1184, doi:10.1130/B25964.1.

Sack, R. O., and M. S. Ghiorso (1991), An internally consistent model for the thermodynamic properties of Fe-Mg-titanomagnetite-aluminate spinels, *Contrib. Mineral. Petrol.*, *106*, 474–505.

Schmidt, M. W. (1992), Amphibole composition in tonalite as a function of pressure; an experimental calibration of the Al-in-hornblende barometer, *Contrib. Mineral. Petrol.*, *110*, 304–310.

Sisson, V. B., and T. C. Onstott (1986), Dating blueschist metamorphism: A combined $^{40}Ar/^{39}Ar$ and electron microprobe approach, *Geochim. Cosmochim. Acta*, *50*, 2111–2117.

Tatsumi, Y., M. Sakuyama, H. Fukuyama, and I. Kushiro (1983), Generation of arc basalt magmas and thermal structure of the mantle wedge in subduction zones, *J. Geophys. Res.*, *88*, 5815–5825.

Winkler, G. R. (1992), Geologic map and summary geochronology of the Anchorage 1° × 3° quadrangle, southern Alaska, *U. S. Geol. Surv. Misc. Invest. Ser. Rep.*, *I-2283*, scale 1:250000.

Winkler, G. R., M. L. Silberman, A. Grantz, R. J. Miller, and E. M. MacKevett Jr. (1981), Geologic map and summary geochronology of the Valdez quadrangle, southern Alaska, *U. S. Geol. Surv. Open File Rep.*, *80-892-A*, scale 1:250000.

Yamamoto, H., and T. Yoshino (1998), Superposition of replacements in the mafic granulites of the Jijal Complex of the Kohistan Arc, northern Pakistan: Dehydration and rehydration within deep arc crust, *Lithos*, *43*(4), 219–234.

Yoshino, T., and T. Okudaira (2004), Crustal growth by magmatic accretion constrained by metamorphic P-T paths and thermal models of the Kohistan Arc, NW Himalayas, *J. Petrol.*, *45*(11), 2287–2302.

Yoshino, T., H. Yamamoto, T. Okudaira, and M. Toriumi (1998), Crustal thickening of the lower crust of the Kohistan Arc (N. Pakistan) deduced from Al zoning in clinopyroxene and plagioclase, *J. Metamorph. Geol.*, *16*(6), 729–748.

M. D. Behn and L. Mehl, Woods Hole Oceanographic Institution, Woods Hole, MA 02543, USA. (mbehn@whoi.edu; lmehl@whoi.edu)

B. R. Hacker, Department of Earth Science, University of California, Santa Barbara, CA 93106, USA. (hacker@geol.ucsb.edu)

P. B. Kelemen, Columbia University, P.O. Box 1000, Palisades, NY 10964, USA. (peterk@ldeo.columbia.edu)

P. Luffi, Department of Earth Science, Rice University, MS-126, 6100 Main Street, Houston, TX 77005-0000, USA. (pluffi@rice.edu)

M. Rioux, Department of Earth, Atmospheric and Planetary Sciences, Massachusetts Institute of Technology, 77 Massachusetts Avenue, Cambridge, MA 02139-0000, USA. (riouxm@mit.edu)